Author Response on "Biogeochemical protocols and diagnostics for the CMIP6 Ocean Model Intercomparison Project (OMIP)"

James C. Orr[1], Raymond G. Najjar[2], Olivier Aumont[3], Laurent Bopp[1], John L. Bullister[4],
Gokhan Danabasoglu[5], Scott C. Doney[6], John P. Dunne[7], Jean-Claude Dutay[1], Heather Graven[8],
Stephen M. Griffies[7], Jasmin G. John[7], Fortunat Joos[9], Ingeborg Levin[10], Keith Lindsay[5],
Richard J. Matear[11], Galen A. McKinley[12], Anne Mouchet[13,14], Andreas Oschlies[15],
Anastasia Romanou[16], Reiner Schlitzer[17], Alessandro Tagliabue[18], Toste Tanhua[15], and Andrew Yool[19]

[1]LSCE/IPSL, Laboratoire des Sciences du Climat et de l'Environnement, CEA-CNRS-UVSQ, Gif-sur-Yvette, France
[2]Dept. of Meteorology, Pennsylvania State University, University Park, Pennsylvania, USA
[3]Laboratoire d'Océanographie et de Climatologie: Expérimentation et Approches Numériques, IPSL, Paris, France
[4]Pacific Marine Environmental Laboratory, NOAA, Seattle, Washington, USA
[5]National Center for Atmospheric Research, Boulder, Colorado, USA
[6]Marine Chemistry & Geochemistry, Woods Hole Oceanographic Institution, USA
[7]NOAA Geophysical Fluid Dynamics Laboratory, Princeton, New Jersey, USA
[8]Dept. of Physics, Imperial College, London, UK
[9]Climate and Environmental Physics, Physics Inst. & Oeschger Center for Climate Change Res., Univ. of Bern, Switzerland
[10]Institut fuer Umweltphysik, Universitaet Heidelberg, Heidelberg, Germany
[11]CSIRO Oceans and Atmosphere, Hobart, Tasmania 7000, Australia
[12]Atmospheric and Oceanic Sciences, University of Wisconsin-Madison, Wisconsin, USA
[13]Max Planck Institute for Meteorology, Hamburg, Germany
[14]Astrophysics, Geophysics and Oceanography Department, University of Liege, Liege, Belgium
[15]GEOMAR Helmholtz Centre for Ocean Research Kiel, Kiel, Germany
[16]Columbia University and NASA-Goddard Institute for Space Studies, New York, NY, USA
[17]Alfred Wegener Institute, Bremerhaven, Germany
[18]Earth, Ocean and Ecological Sciences, University of Liverpool, Liverpool, UK
[19]National Oceanographic Centre, Southampton, UK

Correspondence to: James Orr (james.orr@lsce.ipsl.fr)

We thank the two referees and the three contributors of short comments for their many thoughtful remarks, which together have improved the manuscript. These comments are repeated below in gray, our first responses follow in black, and our final response and changes to the manuscript are indicated in blue.

5 **Response to Comment from Anonymous Referee #1**

This paper lays out a strategy for the biogeochemistry component (OMIP-BGC) of the Ocean Model Intercomparison Project under the umbrella of the 6th Coupled Model Intercomparison Project (CMIP6). The paper is well written and mostly does a good job of outlining the experimental design for potential participants in clear and unambiguous terms. The promised OMIP-

BGC web page (bottom p. 19) does not appear to be operational yet (and rather more than 4 weeks have passed).

Thanks. There now exists an unreleased OMIP-BGC web page. It will be made available once the initialization data sets are finalized, within 15 days after this revised manuscript is submitted. We are sorry for this delay, but the OMIP-BGC web page will go online before this revised paper has a chance to be published.

Major comments:

Overall strategy and ordering of priorities

The weakest point of the strategy is that it is vague about the priority of experiments. In CMIP5, there were tiers of experiments (Core/Tier1/Tier2), and tiers of output fields (Priority 1/2/3). This document does not really separate the two, implicitly treating all experiments as Core. The list of Priority 1 output fields is expansive and probably unrealistic.

We agree that a weak point of the manuscript is that the priority of experiments is not as clear as it should be. In the revised manuscript, we will strive to improve this deficiency, following these comments and Short Comments from others.

The revised manuscript is clearer about the experiments, using Tier 1 to indicate the required simulation *(omip1)* and Tier 2 to indicate the optional simulation *(omip1-spunup)*. Furthermore, Priorities 1, 2, and 3 are indicated in the diagnostic tables.

Some tracers are referred to as "level=1" and "level=2" (5/25), but the term is not defined. It appears to refer to output fields in which case it is synonymous with "Priority" (Tables 4-14) and there is no real conceptual problem. But the most important thing the authors need to do is to separate the x (experiments) and y (output fields) axes in a fashion similar to the CMIP5 data request, and pare down the list of Priority 1 fields to a more realistic level.

Separating out the experiments and output fields in a clearer fashion is a good idea that we will try to implement in the revised manuscript. In the light of these comments, the coauthors will rediscuss the list for Priority 1 fields.

We have changed "level" to "priority" in this passage. We no longer use level to indicate the priority, anywhere in the revised manuscript. The approved CMIP6 terms to designate the importance of the experiments (Tier) and the output fields (Priority) are now used rigourously throughout the text.

The list of 3D monthly fields is long. In CMIP5 no 3D ocean biogeochemistry fields were monthly. According to Moore's Law, computing power should have increased about 16-fold since CMIP5, but in practice the gain is probably much less. Making previously annual fields monthly requires a twelvefold increase just to break even in terms of the time and storage capacity

it will take to access and download data, even assuming no increase in model resolution.

The lack of 3-D monthly fields below the surface in CMIP5 was an impediment to analysis. We do not wish to repeat that mistake during CMIP6. Monthly fields will be valuable to the community, and cutting back on requested fields will limit the science that can be done. See also the comments from Referee #2 along the same lines. Those that do not wish to analyze the monthly fields may choose to download and analyze only the annual mean fields.

After discussion among coauthors, we now list only four required 3-D fields to be stored at monthly frequency (Priority 1). All other 3-D fields have been demoted to Priority 2 (optional). To partially compensate, we ask for surface monthly concentrations (Priority 1) for the demoted 3-D tracer fields.

For any model that includes feedbacks between saturation state and biology, the duplication of tracers is likely to make the 'natural CO2' experiments prohibitively expensive. Yet these are said in the Conclusion to be critical (19/14) and to be "required" on 6/19. Even if one only considers the effect of saturation state on dissolution of CaCO3, that is a minimum of three additional tracers (or maybe two if CaCO3 is parameterized). I agree with the authors that these experiments are important, but the rather superficial consideration given to the actual cost (bottom p. 6) simply underscores that the strategy does not include a clear hierarchy of priorities for the different experiments proposed.

In defense of the original manuscript, adding three passive tracers in an online coupled physical-biogeochemical simulation does not typically increase costs greatly, far less than a factor of two. In such models, the computational cost of running the dynamical model typically dominates. If a separate simulation needs to be run for the natural component, then of course that would double the computational time. But the only required simulation (ocmip1) is initialized from data and run for 310 years. These forced ocean simulations being proposed for OMIP are much less computationally expensive than are the Earth System Model simulations at the same resolution. Nonetheless, we agree that a clearer strategy needs to be elaborated, an effort we will take on with the revised manuscript.

We have adapted the wording of the two sentences to be less emphatic; however, we still consider the natural carbon tracer to be crucial to eliminate model drift.

Alkalinity and speciation

I agree that using a truncated expression for alkalinity causes large errors, but the paper could spell out in detail exactly what they envision alkalinity as including (since the full formal definition includes lots of species that are not provided in a model simulation), rather than simply referring the reader to the provided codes.

The revised manuscript will include the equation for total alkalinity that is provided already in the common code for computing the carbonate chemistry (mocsy). This equation is also provided in the publication which describes that code (Orr and Epitalon, 2015, Equation 7).

5   The revised manuscript now includes an equation that lists all components of total alkalinity that are recommended to be included in the OMIP simulations (equations 32–38

Similarly, the authors could clarify exactly what they mean by N speciation (18/14). I agree that the alkalinity sources and sinks associated with biological transformations (e.g., nitrification) of N species should be accounted for. But I think it is better
10   if the word speciation is not used here.

Good point. The revised manuscript will clarify this issue, avoiding the word speciation.

We avoid the term "nitrogen speciation" in the revised manuscript. Instead we use the term "different inorganic forms of
15   nitrogen"

For models that have N but not P it is recommended that the PO4 contribution to alkalinity be calculated as the P/N Redfield ratio times the total inorganic N concentration (16/29), which is appropriate. But then on 18/15-16 this is referred to as the effect of nitrate on alkalinity. But really what is being referred to here is the effect of phosphate on alkalinity, parameterized as DIN/16. How much N is present as e.g. NO3 vs NH4 is not relevant.

20

Thanks for pointing out this confusing passage. It will be clarified in the revised manuscript.

Our intent concerning the sentence on 18/15-16 was not to account for the effect of phosphate. Rather it was to account for the effects of the different inorganic forms of nitrogen on alkalinity. Indeed, their effects differ as a function of their form as
25   detailed by Wolf-Gladrow et al. (2007). That sentence has now been replaced with "Models with P_T as the sole macronutrient tracer should consider accounting for the effect of nitrate assimilation and remineralization on alkalinity, effects that are 16 times larger than for those for P_T (Wolf-Gladrow et al., 2007)."

It might be useful to include a table of the net alkalinity change associated with biological transformations of N (phyto-
30   plankton uptake, remineralization, nitrification, denitrification, N2 fixation), to help ensure that this is done consistently across models. These numbers can be found in Wolf-Gladrow et al 2007 Mar Chem 106: 287. I think such a table would be more useful than Figure 3, which I do not think is necessary.

Thank you for this idea to include a table of net alkalinity changes due to biological transformations of nitrogen. We will
35   consider this for the revised manuscript. As for Fig. 3, that presents the speciation of phosphoric acid and silicic acid species

as a function of pH. It is not directly related to transformations of nitrogen. We think it adds value to the manuscript because it clarifies what species are important. There is a common misconception among many ocean scientists who refer to phosphate (PO_4^{3-}) when what they really should refer to is the total dissolved inorganic phosphorus (P_T). Even the publications and web pages that describe the World Ocean Atlas incorrectly refer to phosphate when in fact the discrete and objectively mapped data is actually P_T. Eliminating this confusion seems to us to be valuable for the ocean modeling community as well as others.

The Table by Wolf-Gladrow et al. (2007) is interesting and we now cite that publication in the revised manuscript when mentioning the need to account for effects from nitrogen on alkalinity. We stop short though of republishing the same table in our revised manuscript. Yet we do not wish to remove Figure 3 from the revised manuscript because our bjerrum plot for the phosphoric acid system differs from that provided by Wolf-Gladrow et al. (2007). Indeed our curve for HPO_4^- shows a peak around the pH of surface seawater, while the same curve in Figure 3 of Wolf-Gladrow et al. (2007) exhibits a plateau that extends from pH 8 to pH 12. That difference arises because Wolf-Gladrow et al. uses values for pK1, pK2, and pK3 of the phosphiric acid system that are appropriate for pure water; conversely, we use values that are appropriate for seawater.

I also note that Fe speciation is far more complex than implied in Footnote 2 to Table 5, so that it might be better to simply state that modelled dFe includes all dissolved species. Also Fe* (column 1) is not defined, assuming that the * is not just an erroneously placed footnote marker.

The revised manuscript will attempt to clarify these concerns about dissolved iron.

We have changed the footnote to "modeled dissolved iron includes all simulated dissolved species, both free and organically complexed". The "*" should have pointed to the footnote that describes the meaning of dissolved iron; it now does so in the revised manuscript.

Minor comments

Is "online" rather than "in line" the proper terminology? In any case the authors should define it at first occurrence.

We may be confused about the meaning this comment. As we do not use the term "in line", is the Referee suggesting that we replace all occurrences of "online" with "in line"? This is not what we wish to do. Online has a particular meaning in the ocean modeling world. Perhaps though, the Referee is suggesting that we should define "online" when it is first used. Such will be done in the revised manuscript.

We now define online when it is first used (in the Introduction).

2/23 change "model-predicted" to "modelled"

In the revised manuscript, we have changed "model-predicted" to "simulated".

7/32 "Carbon-13 is typically included in ocean models as a biotic variable influenced by fractionation effects during photosynthesis that depend on growth rate and phytoplankton type." could use some literature references.

In the revised manuscript, we have added one reference (Tagliabue and Bopp, 2008).

8/25-30 Might want to mention here that while the equilibration times for Fe and DOC are much longer than for e.g. phytoplankton biomass, they are much shorter than for DIC or alkalinity.

We prefer not to make this statement in the revised manuscript. Although true, it distracts from the paragraph's topic, which is about how to initialize tracer fields, not their equilibration time.

9/18 not clear what the stray < means

This was a typo. It has been removed in the revised manuscript.

12/20 "polynomical"???

Another typo. It has been corrected to "polynomial".

12/27-28 change "pH2O is the water vapor pressure at saturation" to "pH2O is the saturation vapor pressure at sea surface temperature and salinity" (see 15/26)

In the revised manuscript, we have changed the wording to the "pH2O is the vapor pressure of water (also in atm) at sea surface temperature and salinity". The term "vapor pressure of water" is exactly the phrasing used by Weiss and Price (1980).

16/18-21 The authors recommend that carbon chemistry calculations follow the Best Practices Guide (Dickson et al., 2007). They might also consider mentioning that the BPG also gives formulae for the coefficients in equation (26). Interestingly, the definition of R used here differs slightly (1e-6 level) from that in the BPG.

The original reference is Weiss (1974). We may add a reference to the BPG in the revised manuscript. The value of R has been updated since the best-practices guide was published 10 years ago.

We cite the original reference (Weiss, 1974); the BPG refers to the same coefficients (from Weiss) for B and their version of equation (26) is identical. The value of R that we refer to here is from CODATA(2006) of the NIST. The slight difference does not lead to significant differences in model calculations.

17/5 delete the '*' in equation 27

This sign was indeed unnecessary. It has been removed in the revised manuscript.

Table 5 "Mole concentration of phytoplankton expressed as chlorophyll" I think just "Concentration of chlorophyll" is more accurate (see Table 9). I also don't think the second sentence of the footnote is necessary.

In the revised manuscript, Table 5 will list the name of this variable exactly as it is given in the CMIP6 data request.

That entry in Table 5 has now been changed to "Mass Concentration of Chlorophyll in Seawater". More generally, much work has gone into revising the tables to make descriptions clearer and consistent with the CMIP6 MIP Table for OMIP.

Response to Comment from Anonymous Referee #2

This manuscript presents a plan for simulations and diagnostics of biogeochemical tracers during the CMIP6 simulations, including carbon cycle and biological tracers. Model intercomparison projects are somewhat unwieldy beasts, when comparing models it is often difficult to know what to say beyond "the models differ". Reasons for this include subtle differences in model construction and parameter values as well as more fundamental issues about which processes are represented. Ideally, model intercomparison projects will try to keep as many things as similar as possible, so as to narrow down the range of possible differences between simulations. The strategy taken in this version of CMIP seems to be to make sure the different models all use the same gas exchange, atmospheric concentration, gas chemistry and carbon chemistry parameters, while using different ecosystem models. This seems a very sensible approach to me.

We agree. Physical forcing of the ocean only model simulations will also be identical.

It would be good at the end of the introduction for the authors to define what the principal scientific goals are. Right now it appears that a principal goal is to quantify the change in ocean carbon inventory under global warming and to attribute this uptake to passive uptake by a changing circulation vs. changes in the natural storage of carbon by biology. It would be good to say a little more about why this is challenging, in particular that the long equilibration time for carbon dioxide means that the (poorly known) disequilibrium component of anthropogenic CO_2 is the same size as the actual signal we are trying to detect.

As a result, different estimates of anthropogenic CO2 differ by large amounts. Combining C14 with SF6 and CFC12 tracers offers us a way of not only testing the models, but of narrowing the observational uncertainty on anthropogenic CO2. However, doing this right requires not only getting inventories but fluxes right, which in turn requires standardizing carbon chemistry (the recent paper by Lovenduski et al in Global Biogeochemical Cycles would be a good one to reference here as it shows that systematic model bias dominates regional carbon fluxes). This would motivate the discussion later in the paper.

In the revised manuscript, the main scientific goals of the project will be better detailed as also requested in the short comment from the CMIP Panel. Referee #2 provides valuable suggestions, including the interesting reference to the work by Lovenduski et al. (2016), which we plan to address in the revised manuscript.

To better detail the scientific goals of OMIP-BGC, the final paragraph of the Introduction of the submitted manuscript has been modified, and two new paragraphs have been added just afterwards. The reference suggested by Referee #2 has been cited.

Additionally however, biogeochemical tracers can serve as useful constraints on ocean circulation, in particular the ventilation of the deep ocean, as they average over long periods of time and exhibit strong contrasts between different regions of deep water formation. A great example of this is Broecker et al. (JGR-Oceans) use of C14 and PO4* to derive ventilation rates for Antarctic Bottom Water and North Atlantic Deep Water—the former of which is likely still better than anything that physical oceanographers have been able to quantify directly. Radiocarbon is also useful for getting at upwelling pathways, as different overturning schemas can produce vastly different distributions of surface radiocarbon with very similar overall hydrography (see Gnanadesikan et al., GBC, 2004 for an example of this).

The utility of the tracers that will be modeled in the OMIP-BGC simulations to help constrain ocean circulation, particularly in the deep ocean, will be brought forward in the Introduction to help emphasize these objectives. The publications suggested by Referee #2 (Broecker et al., 1998; Gnanadesikan et al., 2004) are excellent examples that we will consider mentioning in the revised Introduction.

In the submitted manuscript, the Introduction already mentioned that ^{14}C is used to assess subsurface ventilation times. However, we follow Referre #2's advice, emphasizing this point further in ther revised manuscript by also mentioning the study by (Broecker et al., 1998).

Finally, though, there's the issue of biological variability under climate change. This will be an important area going forward and I do not feel that the diagnostics for it have been properly prioritized. One of the main "consumers" of this work are going to be marine ecologists looking for changes in community structure and ecology. Because of this I would strongly recommend prioritizing monthly 100m-integrated biomass measurements for as many classes as exist in the model as a top priority. I disagree with the reviewer who worried about having too many diagnostics- frankly the field as a whole suffers from

having too few diagnostics saved out to actually understand differences. In the current version of CMIP5, for example, many of the models save out minimum oxygen rather than the three-dimensional fields. In analysing this my group is finding that this limits the signals of changes in climate to convective zones, rather than allowing them to be tracked more broadly.

5   Agreed. The requested monthly fields will be valuable contributions that OMIP and CMIP6 can provide to help offer a better understanding of biological and chemical variability and potential changes under climate change and rising levels of CO_2.

In the revised manuscript, we still request monthly tracer fields also in subsurface waters (i.e., monthly 3-D fields), but in response to Referee #1 the Priority for most of those fields has been lowered from 1 (required) to 2 (optional).

10

I have only one other quibble about the standards. The OCMIP2 standards for carbon and radiocarbon were generally for models that did not have interannual variability but were being forced towards a mean climate. When climate variability is included (and as noted by de Lavergne et al., 2015 this variability can have large amplitude) one can easily see variability accounting for differences of 5 GtC over the course of a century. I strongly recommend that the authors either raise the threshold

15 for carbon trends or soften the requirement in some way.

We are not sure that we fully understand the meaning of this comment nor the exact publication that is being referred to. The OMIP-BGC models will account for climate variability, either when forced by reanalysis data or when coupled within an Earth System Model framework. The boundary condition for atmospheric CO_2 does include interannual variability, being based on

20 annual-mean observations. The same may be said for the atmospheric $^{14}C/C$ ratio. Furthermore given the corresponding air-sea equilibration times (1 yr and 10 yr, respectively) it is not clear to us that the atmospheric records that are to be used to force the OMIP-BGC simulations are inadequate to study interannual variability. More clarification from Referee #2 on the nuanced meaning of this comment would be most welcome.

25 No changes were made to the submitted manuscript regarding this point because we already account for climate variability in the OMIP protocols, unlike for OCMIP2.

Response to Short Comment by N. Swart

Firstly, thanks to the authors for coordinating the OMIP-BGC effort and putting together this very comprehensive document-

30 ing paper. I have a few comments, which I think will be relevant to modelling centres trying to perform the simulations and diagnostics you describe:

- For the diagnostic output (section 3 and tables 9 to 14), no indication is given on which variables are expected only for the OMIP-BGC ocean model runs; and which variables are expected from the Earth System Models doing the "full" CMIP6 runs (historical etc), unless I missed this somewhere. It would be good to mark clearly if there are variables expected only for OMIP-BGC runs, but not the rest of CMIP6.

5

Conceptually there is no difference in output requirements for the forced ocean simulations made for OMIP and the coupled simulations made with the Earth System Models that are participating in CMIP6. These simulations differ in forcing but not in the types of output requested. However, we will further consider this point and clarify when distinguishing the two types of simulations in the revised manuscript.

10

The first two sentences in our response just above are now included in Section 3 of the revised manuscript.

- Table 5 and 9 mark all variables as "priority 1". My understanding of a priority 1 variable is from the CMIP6 data request: "all participating groups must commit to supplying all priority 1 variables". Thus, priority 1 variables should be the lowest

15 common denominator that all groups can provide. In tables 5 and 9, there are multiple variables (like 13C, and all the "abiotic" terms) which are not carried in all (or even most) BGC models. Thus, groups face the significant coding and computation expense of adding 7+ new tracers if they are "required" to provide all these terms to participate in OMIP-BGC. If these variables are not indeed "required", please mark them as priority 2, in which case it is clear they can be provided optionally, if available. Otherwise, as I understanding it, any group not providing all these variables will end up not "participating" [at least officially].

20

These are excellent points. Priorities will be clarified following the CMIP6 data request for OMIP that has been refined since the original manuscript was submitted. Priorities will be adjusted and explained in detail, following the CMIP6 guidelines.

Motivated by these remarks, much discussion ensued among coauthors. This has led to substantial changes to the Diagnostic

25 tables. The priorities for the monthly 3-D fields has generally been lowered from 1 to 2. Tables 5 and 9 list fewer tracers, including only those that all model groups will be able to contribute.

In the revised manuscript we will also make it clearer that $\delta^{13}C$ simulations are recommended only for those who already have experience modeling this tracer. The abiotic tracers are highly recommended but not required for participation in OMIP.

30 Fortunately, many modeling groups already have experience simulating abiotic dissolved inorganic carbon and radiocarbon, and for those that do not, their addition as new tracers is straightforward.

We have now added the following 3 sentences to the subsection on C-13: "Groups that have experience modeling ^{13}C in their biogeochemical model are requested to include it as a tracer in the OMIP-BGC simulations. Groups without experience should avoid adding it. Groups may participate in OMIP without including ^{13}C as a tracer."

35

Response to Short Comment by T. Lovato

This Short Comment is repeated below in gray; our response follows in black. We thank Tomas Lovato for these helpful comments.

5   This manuscript documents the experimental protocol for the biogeochemical and inert chemical tracers under the CMIP6 Ocean Model Intercomparison Project (OMIP), here referred as OMIP-BGC. The description of simulations protocols, preferred parameterizations, and diagnostics is very thorough and it provides a good guidance for all the groups involved in this intercomparison exercise. I have few comments on aspects related to the protocol definition.

10   1- At the beginning of section 2, authors strongly advise to use the constants recommended in best practices described by Dickson (2010). However, Orr and Epitalon (2015) clearly pointed out that some exceptions to the best practices might become relevant when dealing with numerical models. I think that the protocol could be revised by pointing out the use of more suitable parameterizations, like e.g. K1-K2 from Millero (2010) and KF formulation in Dickson and Riley (1979).

15   These points will be addressed more thoroughly in the revised manuscript. Orr and Epitalon (2015) do discuss the Millero (2010) formulations for K_1 and K_2 relative to those recommended for best practices. However, the companion paper (Orr et al., 2015) identified internal discrepancies with the Millero (2010) formulations, recommending to remain with the best-practice formulations until those discrepancies are resolved. We will provide an updated analysis of this situation for K_1 and K_2 in the revised manuscript. Regarding K_F, the choice between the two available formulations (Dickson and Riley, 1979; Perez and 20 Fraga, 1987) does not make a significant difference in computed variables (Dickson et al., 2007; Orr et al., 2015). Indeed some of the public software packages that make these carbonate chemistry calculations (e.g., various versions of CO2SYS) do not even offer a choice.

    Given the statements in our first response above, we stand by our choice to recommend that modelers use all the constants 25 recommended for best practices Dickson et al. (2007); Dickson (2010). We have not changed the revised manuscript in this regard.

    2- The protocol for simulations indicates that initial conditions for DIC an TA are based on the recent GLODAPv2 (see section 2.2). In particular, these data are provided over two distinguished time periods, namely from 1986–1999 for the WOCE 30 era and from 2000-2013 for the CLIVAR one (see Key et al., 2015). It would be very useful to report in the manuscript how these data will be handled to create the initial conditions (use only one period, data blending, etc.), especially if one consider that DIC is remarkably time-dependent over long time windows.

In theory, either the first or second period could be used for initial conditions if pre-treatment of the GLODAPv2 data would include removing the anthropogenic DIC component (or part of it) based on data-based estimates (e.g., Khatiwala et al., 2009). The revised manuscript will discuss this point and stipulate the preferred option.

5   In the revised manuscript, we now write, "For greater consistency with GLODAPv1, OMIP-BGC model groups will use the C_T and A_T fields from GLODAPv2's first period (1986–1999, the WOCE era)."

    3- In section 2.5.3, it is indicated that in-situ temperature and salinity in permil units have to be used in the computations related to the carbonate system. I think that the preferred type of these two variables could be addressed more precisely, e.g. in 10 situ temperature as ITS-90 and Practical Salinity as PSS-78, also to comply with the routines used in mocsy.

    These specifications of the T and S scales have been added to the revised manuscript.

    4-In the companion paper on OMIP physical experiments (Griffies et al., 2016) it is considered also the use of most recent 15 Equation of State for ocean physics (TEOS-10), which relies on Conservative Temperature and Absolute Salinity. This might represent a critical issue since equilibrium constants were all derived using practical salinity (Millero, 2007; Dickson, 2010). I guess that some guidelines on the use of the most appropriate conversions tools between different formulations of temperature and salinity should be addressed in the protocol description.

20   For these conversions, the revised manuscript will recommend that model groups should use the routines from the TEOS-10 Fortran library, available from http://www.teos-10.org/software.htm.

    In section 2.6 of the revised manuscript, we have added the following "Although by default *mocsy* uses older scales for temperature and salinity (ITS90 and PSS78, respectively) for input, the latest version now includes a new option so that modelers 25 can choose to use the new TEOS-10 standards (Conservative Temperature and Absolute Salinity)."

    5- I think it would be very useful to have a table that summarizes the requested variables for each Tier and link them to the specific experiments of both OMIP-BGC and DECK.

30   We will consider this as an option for the revised manuscript while weighing the concern of excessive duplication. The publicly available CMIP6 data-request tables for OMIP will contain the same information and can be sorted by individual modeling groups according to their needs.

    As we already have 16 Tables in the revised manuscript, it would be unwise to add more. However, we do plan to add the 35 link fot the final OMIP MIP tables (Excel spreadsheets) to the OMIP-BGC web page, so that modelers can download those

Key, R.M., A. Olsen, S. van Heuven, S. K. Lauvset, A. Velo, X. Lin, C. Schirnick, A. Kozyr, T. Tanhua, M. Hoppema, S. Jutterström, R. Steinfeldt, E. Jeansson, M. Ishi, F. F. Perez, and T. Suzuki. 2015. Global Ocean Data Analysis Project, Version 2 (GLODAPv2), ORNL/CDIAC-162, ND-P093. Carbon Dioxide Information Analysis Center, Oak Ridge National Laboratory, US Department of Energy, Oak Ridge, Tennessee. doi:10.3334/CDIAC/OTG.NDP093_GLODAPv2.

Response to Short Comment by C. Senior, representing the CMIP Panel

The CMIP Panel is undertaking a review of the CMIP6 GMD special issue papers to ensure a level of consistency in answering the key questions that were outlined in our request to submit a paper to all co-chairs of CMIP6-Endorsed MIPs. These questions are outlined in the overview paper (Eyring et al, GMD, 2016) and the relevant section is summarised below:

Each of the 21 CMIP6-Endorsed MIPs is described in a separate invited contribution to this Special Issue. These contributions will detail the goal of the MIP and the major scientific gaps the MIP is addressing, and will specify what is new compared to CMIP5 and previous CMIP phases. The contributions will include a description of the experimental design and scientific justification of each of the experiments for Tier 1 (and possibly beyond), and will link the experiments and analysis to the DECK and CMIP6 historical simulations. They will additionally include an analysis plan to fully justify the resources used to produce the various requested variables, and if the analysis plan is to compare model results to observations, the contribution will highlight possible model diagnostics and performance metrics specifying whether the comparison entails any particular requirement for the simulations or outputs (e.g. the use of observational simulators). In addition, possible observations and reanalysis products for model evaluation are discussed and the MIPs are encouraged to help facilitate their use by contributing them to the obs4MIPs/ana4MIPs archives at the ESGF (see Section 3.3). In some MIPs additional forcings beyond those used in the DECK and CMIP6 historical simulations are required, and these are described in the respective contribution as well.

We very much welcome the OMIP BGC contribution and the hugely valuable detailing of the desired formulations for gas exchange and carbonate chemistry, diagnostic tracers and their initialisation that you currently cover in section 2. This is nicely consistent with the leadership that the other OMIP paper (Griffies et al) is also providing on the physical ocean diagnostics and together these will provide an important protocol for CMIP6.

Thank you.

However we would like to suggest that for consistency with the other papers in the GMD special issue, you consider moving much of section 2 to an appendix rather than in the main body of the paper. A similar suggestion was made on the Griffies at

13

al paper for documentation of diagnostics. Some parts of section 2 such as detailing the tier 1 experiments, their length and initialisation should remain in the main paper and perhaps this section can be re-organised around these including the justification of these runs. I think much of this is already in the paper but could be better structured.

5   The question of moving some of information on protocols to an appendix will be considered. However, we fear that a reorganization that would break apart the protocols into two major sections (one being an appendix), separated by other sections, would force readers to need to repeatedly move back and forth between sections, degrading flow. However during the revision process, we will more fully consider this option.

10   We agree that moving a specialized section from the main body to an appendix is often a good way to to streamline a paper. We have made an attempt to do this, but the result was unsatisfactory. The problem is that the section that is mentioned (Protocols) is the main section of our paper. If all of it were moved to an appendix, only 3 or 4 pages of text would remain for the main body. If part of it were moved, the targeted readers (mostly ocean biogeochemical modelers) would need to move back and forth across many other sections many times when studying the protocols. Furthermore, we fear that relegating the
15   protocols to an Appendix might be taken as a sign by some readers that it is optional material that does not need close attention. Therefore we have kept the Protocols section in the main body of the paper.

      Additionally, we would like to see some more detail on some of the issues raised above, notably;

20   a. More discussion on the science goals of the OMIP BGC in CMIP6 and what science gaps it is attempting to fill to be outlined in the introduction. You mention that OMIP BGC is focussed on the CMIP6 question on 'understanding systematic biases' but give no detail on what OMIP BGC is hoping to achieve that is new.

      In the revised manuscript we will include more detail on the OMIP-BGC science goals as well as the gaps to be addressed.
25   We will then further address how OMIP-BGC aims to assess fundamental concerns about systematic biases.

      In the revised manuscript, more information on the science goals, the gaps to be addressed, and new achievments are provided in the final three paragraphs of the Introduction. Two of them are new; the other has been revised.

30   b. All MIPs have been asked to demonstrate connectivity to the DECK experiments and the CMIP6 historical simulations as one of the 10 endorsement criteria (see Table 1 in Eyring et al., 2016). Please document this for OMIP BGC.

      The connectivity to the CMIP6 historical and DECK experiments will be made clearer in the revised manuscript.

14

We have inserted a paragraph in the first part of the Protocols section, that describes the connectivity between the OMIP simulations and CMIP6 DECK and historical simulations.

c. You have not provided an analysis plan for the science community engaged in OMIP BGC. How are you going to use the experiments and diagnostics? Are you committing to analyse all the data that you are requesting (or can you point to other MIPs that will do so)?

The OMIP-BGC effort aims to provide a central forum to promote discussion, facilitate analysis, and prompt wide participation of the ocean biogeochemical modeling community in the related analysis effort. In this sense then, speaking for the community, the goal is indeed to analyze all of the model output requested. An analysis plan will be included in the revised manuscript. Other MIPs under the CMIP6 umbrella such as C4MIP will certainly take on some analysis of ocean output for which OMIP has provided diagnostics.

A short paragraph has been added at the end of the Diagnostics section in order to provide a glimpse of how we aim to proceed in order to promote analysis within the international community.

d. You describe observations of e.g. CFC-11, CFC-12, SF6 etc in the introduction that might be used for evaluation of the models. Are/Could any new observations be made easily available to the modelling community (e.g. through Obs4MIPs?)

Discrete and gridded observations of CFC-11, CFC-12, and SF_6 will be used extensively to evaluate the OMIP models. Whether we have the right, as a modeling community, to submit new observations through Obs4MIPs is an open question that we have not adequately considered. Certainly existing observations that are already available publicly could also be added through Obs4MIPS, assuming approval can be obtained from the data providers. It is an aim of OMIP-BGC to facilitate access to the relevant observational data that is used for model evaluation, as done previously during the Ocean Carbon Cycle Model Intercomparison Project.

We intend to explore these possibilities in the future, but for now our understanding is too preliminary concerning the possibilities and legal impediments to contributing to contributing to Obs4MIPs. Hence we have added nothing to the manuscript about this future possibility.

We hope you agree that some level of consistency across the MIP papers in this special issue is valuable and that the above suggestions can be accommodated in your paper.

Consistency across the contributions to the CMIP6 special issue in GMD is important, and we will do our part to help.

Other comments:

- For the diagnostic section (3 and tables 4-14), what is the link to the CMIP6 data request? Perhaps you need to clarify where is the definitive documentation of what is actually being output from the models (e.g. via a link to the actual data request) and to reference the GMD paper by Martin Jukes?

In the revised document, we plan to cite the GMD paper by Jukes and provide links to the CMIP6 data request, while assuring consistency with revisions to the Tables.

Unfortunately, we were unable to find any publication in GMD by Martin Juckes et al. However, we have indicated the link to the CMIP6 data request in the Diagnostics section of our revised manuscript.

Other comments: With many thanks for your ongoing efforts in the CMIP6 process.

The CMIP Panel

Your comments are much appreciated.

References

Broecker, W., Peacock, S., Walker, S., Weiss, R., Fahrbach, E., Schröder, M., Mikolajewicz, U., Heinze, C., Key, R., Peng, T.-H., et al.: How much deep water is formed in the Southern Ocean?, Journal of Geophysical Research: Oceans, 103, 15 833–15 843, 1998.

Dickson, A. G.: The carbon dioxide system in seawater: equilibrium chemistry and measurements, in: Guide to best practices for ocean acidification research and data reporting, edited by Riebesell, U., Fabry, V. J., Hansson, L., and Gattuso, J.-P., pp. 17–40, Publications Office of the European Union, 2010.

Dickson, A. G. and Riley, J. P.: The estimation of acid dissociation constants in seawater media from potentiometric titrations with strong base. I. The ionic product of water - K_W, Mar. Chem., 7, 89–99, 1979.

Dickson, A. G., Sabine, C. L., and Christian, J. R.: Guide to best practices for ocean CO_2 measurements, , PICES Special Publication 3, 191 pp., http://aquaticcommons.org/1443/, 2007.

Gnanadesikan, A., Dunne, J. P., Key, R. M., Matsumoto, K., Sarmiento, J. L., Slater, R. D., and Swathi, P.: Oceanic ventilation and biogeo-chemical cycling: Understanding the physical mechanisms that produce realistic distributions of tracers and productivity, Global Biogeo-chemical Cycles, 18, doi:10.1029/2003GB002 097, 1944–9224, 2004.

Khatiwala, S., Primeau, F., and Hall, T.: Reconstruction of the history of anthropogenic CO2 concentrations in the ocean, Nature, 462, 346–349, 2009.

Lovenduski, N. S., McKinley, G. A., Fay, A. R., Lindsay, K., and Long, M. C.: Partitioning uncertainty in ocean carbon uptake projections: Internal variability, emission scenario, and model structure, Global Biogeochemical Cycles, 30, doi:10.1002/2016GB005 426, 1276–1287, 2016.

Millero, F. J.: Carbonate constants for estuarine waters, Mar. Freshwater Res., 61, 139–142, doi:10.1071/MF09254, 2010.

Orr, J. C. and Epitalon, J.-M.: Improved routines to model the ocean carbonate system: mocsy 2.0, Geosci. Model Dev., 8, 485–499, doi:10.5194/gmd–8–485–2015, 2015.

Orr, J. C., Gattuso, J.-P., and Epitalon, J.-M.: Comparison of ten packages that compute ocean carbonate chemistry, Biogeosciences, 12, 1483–1510, doi:10.5194/bg–12–1483–2015, 2015.

Perez, F. F. and Fraga, F.: Association constant of fluoride and hydrogen ions in seawater, Mar. Chem., 21, 161–168, 1987.

Tagliabue, A. and Bopp, L.: Towards understanding global variability in ocean carbon-13, Global Biogeochem. Cy., 22, GB1025, doi:10.1029/2007GB003 037, 2008.

Weiss, R. F.: Carbon dioxide in water and seawater: the solubility of a non-ideal gas, Mar. Chem., 2, 203–215, 1974.

Weiss, R. F. and Price, B. A.: Nitrous oxide solubility in water and seawater, Mar. Chem., 8, 347–359, 1980.

Wolf-Gladrow, D. A., Zeebe, R. E., Klaas, C., Körtzinger, A., and Dickson, A. G.: Total alkalinity: The explicit conservative expression and its application to biogeochemical processes, Mar. Chem., 106, 287–300, 2007.

Biogeochemical protocols and diagnostics for the CMIP6 Ocean Model Intercomparison Project (OMIP)

James C. Orr[1], Raymond G. Najjar[2], Olivier Aumont[3], Laurent Bopp[1], John L. Bullister[4],
Gokhan Danabasoglu[5], Scott C. Doney[6], John P. Dunne[7], Jean-Claude Dutay[1], Heather Graven[8],
Stephen M. Griffies[7], Jasmin G. John[7], Fortunat Joos[9], Ingeborg Levin[10], Keith Lindsay[5],
Richard J. Matear[11], Galen A. McKinley[12], Anne Mouchet[13,14], Andreas Oschlies[15],
Anastasia Romanou[16], Reiner Schlitzer[17], Alessandro Tagliabue[18], Toste Tanhua[15], and Andrew Yool[19]

[1]LSCE/IPSL, Laboratoire des Sciences du Climat et de l'Environnement, CEA-CNRS-UVSQ, Gif-sur-Yvette, France
[2]Dept. of Meteorology, Pennsylvania State University, University Park, Pennsylvania, USA
[3]Laboratoire d'Océanographie et de Climatologie: Expérimentation et Approches Numériques, IPSL, Paris, France
[4]Pacific Marine Environmental Laboratory, NOAA, Seattle, Washington, USA
[5]National Center for Atmospheric Research, Boulder, Colorado, USA
[6]Marine Chemistry & Geochemistry, Woods Hole Oceanographic Institution, USA
[7]NOAA Geophysical Fluid Dynamics Laboratory, Princeton, New Jersey, USA
[8]Dept. of Physics, Imperial College, London, UK
[9]Climate and Environmental Physics, Physics Inst. & Oeschger Center for Climate Change Res., Univ. of Bern, Switzerland
[10]Institut fuer Umweltphysik, Universitaet Heidelberg, Heidelberg, Germany
[11]CSIRO Oceans and Atmosphere, Hobart, Tasmania 7000, Australia
[12]Atmospheric and Oceanic Sciences, University of Wisconsin-Madison, Wisconsin, USA
[13]Max Planck Institute for Meteorology, Hamburg, Germany
[14]Astrophysics, Geophysics and Oceanography Department, University of Liege, Liege, Belgium
[15]GEOMAR Helmholtz Centre for Ocean Research Kiel, Kiel, Germany
[16]Columbia University and NASA-Goddard Institute for Space Studies, New York, NY, USA
[17]Alfred Wegener Institute, Bremerhaven, Germany
[18]Earth, Ocean and Ecological Sciences, University of Liverpool, Liverpool, UK
[19]National Oceanographic Centre, Southampton, UK

Correspondence to: James Orr (james.orr@lsce.ipsl.fr)

Abstract. The Ocean Model Intercomparison Project (OMIP) focuses on the physics and biogeochemistry of the ocean component of Earth System Models participating in the sixth phase of the Coupled Model Intercomparison Project (CMIP6). OMIP aims to provide standard protocols and diagnostics for ocean models, while offering a forum to promote their common assessment and improvement. It also offers to compare solutions of the same ocean models when forced with reanalysis data (OMIP simulations) versus when integrated within fully coupled Earth System Models (CMIP6). Here we detail simulation protocols and diagnostics for OMIP's biogeochemical and inert chemical tracers. These passive-tracer simulations will be coupled ~~online~~ to ocean circulation models, initialized with observational data or output from a model spin up, and forced by repeating the ~~1948-2009~~ 1948–2009 surface fluxes of heat, fresh water, and momentum. These so-called OMIP-BGC simulations include three inert chemical tracers (CFC-11, CFC-12, SF_6) and biogeochemical tracers (e.g. dissolved inorganic carbon, carbon isotopes, alkalinity, nutrients, and oxygen). Modelers will use their preferred prognostic BGC model but should follow common guidelines for gas exchange and carbonate chemistry. Simulations include both natural and total carbon tracers. The required

forced simulation *(omip1)* will be initialized with gridded observational climatologies. An optional forced simulation *(omip1-spunup)* will be initialized instead with BGC fields from a long model spin up, preferably for 2000 years or more and forced by repeating the same 62-year meteorological forcing. That optional run will also include abiotic tracers of total dissolved inorganic carbon and radiocarbon, C_T^{abio} and $^{14}C_T^{abio}$, to assess deep-ocean ventilation and distinguish the role of physics vs. biology. These simulations will be forced by observed atmospheric histories of the three inert gases and CO_2 as well as carbon isotope ratios of CO_2. OMIP-BGC simulation protocols are founded on those from previous phases of the Ocean Carbon-Cycle Model Intercomparison Project. They have been merged and updated to reflect improvements concerning gas exchange, carbonate chemistry, and new data for initial conditions and atmospheric gas histories. Code is provided to facilitate their implementation.

1 Introduction

Centralized efforts to compare numerical models with one another and with data commonly lead to model improvements and accelerated development. The fundamental need for model comparison is fully embraced in Phase 6 of the Coupled Model Intercomparison Project (CMIP6), an initiative that aims to compare Earth System Models (ESMs) and their climate-model counterparts as well as their individual components. CMIP6 emphasizes common forcing and diagnostics through 21 dedicated Model Intercomparison Projects (MIPs) under a common umbrella (Eyring et al., 2016). One of these MIPs is the Ocean Model Intercomparison Project (OMIP). OMIP focuses on comparison of global ocean models that couple circulation, sea-ice, and optional biogeochemistry, which together make up the ocean components of the ~~Earth System Models~~ ESMs used within CMIP6. OMIP works along two coordinated branches focused on ocean circulation and sea ice (OMIP-Physics) and on biogeochemistry (OMIP-BGC). The former is described in a companion paper in this same issue (Griffies et al., 2016), while the latter is described here.

Groups that participate in OMIP will use different ocean biogeochemical models coupled to different ocean general circulation models (OGCMs). The skill of the latter in simulating ocean circulation affects the ability of the former to simulate ocean biogeochemistry. Thus previous efforts to compare global-scale, ocean biogeochemical models have also strived to evaluate ~~model-predicted~~ simulated patterns of ocean circulation. For instance, the Ocean Carbon-Cycle Model Intercomparison Project (OCMIP) included efforts to assess simulated circulation along with simulated biogeochemistry. OCMIP began in 1995 as an effort to identify the principal differences between existing ocean carbon-cycle models. Its first phase (OCMIP1) included four models and focused on natural and anthropogenic components of oceanic carbon and radiocarbon (Sarmiento et al., 2000; Orr et al., 2001). OCMIP2 was launched in 1998, comparing 12 models with common biogeochemistry, and evaluating them with physical and inert chemical tracers (Doney et al., 2004; Dutay et al., 2002; Matsumoto et al., 2004; Dutay et al., 2004; Orr et al., 2005; Najjar et al., 2007). In 2002, OCMIP3 turned its attention to evaluating simulated interannual variability in forced ocean biogeochemical models (e.g. Rodgers et al., 2004; Raynaud et al., 2006). More recently, OCMIP has focused on assessing ocean biogeochemistry simulated by ~~Earth System Models~~ ESMs (e.g. Bopp et al., 2013).

2

OCMIP2 evaluated simulated circulation using the physically active tracers, temperature T and salinity S (Doney et al., 2004), but also with passive tracers, i.e. those having no effect on ocean circulation. For example, OCMIP2 used two anthropogenic transient tracers, CFC-11 and CFC-12 (Dutay et al., 2002). Although these are reactive gases in the atmosphere that participate in the destruction of ozone, they remain inert once absorbed by the ocean. From an oceanographic perspective, they may be thought of as dye tracers given their inert nature and purely anthropogenic origin, increasing only since the 1930s (Fig. 1). Furthermore, precise measurements of CFC-11 and CFC-12 have been made throughout the world ocean, e.g. having been collected extensively during WOCE (World Ocean Circulation Experiment) and CLIVAR (Climate and Ocean— Variability, Predictability and Change). Hence they are well suited for model evaluation and are particularly powerful when used together to deduce decadal ventilation times of subsurface waters. Yet their combination is less useful to assess more recent ventilation, because their atmospheric concentrations have peaked and declined, since 1990 for CFC-11 and since 2000 for CFC-12, as a result of the Montreal Protocol. To fill this recent gap, oceanographers now also measure SF_6, another anthropogenic, inert chemical tracer whose atmospheric concentration has increased nearly linearly since the 1980s. Combining SF_6 with either CFC-11 or CFC-12 is optimal for assessing even the most recent ventilation time scales. Together these inert chemical tracers can be used to assess transient time distributions (TTDs). TTDs are used to infer distributions of other passive tracer distributions, such as anthropogenic carbon (e.g. Waugh et al., 2003), which cannot be measured directly.

To help assess simulated circulation fields, OCMIP also included another passive tracer, radiocarbon, focusing on both its natural and anthropogenic components. Radiocarbon (^{14}C) is produced naturally by cosmogenic radiation in the atmosphere, invades the ocean via air-sea gas exchange, and is mixed into the deep sea. Its natural component is useful because its horizontal and vertical gradients in the deep ocean result not only from ocean transport but also from radioactive decay (half-life of 5700 years), leaving a time signature for the slow ventilation of the deep ocean (roughly 100 to 1000 yr depending on location). Hence natural ^{14}C provides rate information throughout the deep ocean, unlike T and S. For example, the ventilation age of the deep North Pacific is about 1000 years, based on the depletion of its ^{14}C/C ratio (-260‰ in terms of Δ^{14}C, i.e. the fractionation-corrected ratio relative to that of the preindustrial atmosphere) when compared with that of source waters from the surface Southern Ocean (-160‰) (Toggweiler et al., 1989a). In the same vein, ventilation times of North Atlantic Deep Water and Antarctic Bottom Water have been deduced from ^{14}C in combination with another biogeochemical tracer PO_4^* ("phosphate star") (Broecker et al., 1998), facilitated by their strong regional contrasts. The natural component of radiocarbon complements the three inert chemical tracers mentioned above, which are used to assess more recently ventilated waters nearer to the surface. Yet the natural component is only half of the story.

During the industrial era, atmospheric Δ^{14}C declined due to emissions of fossil CO_2 (Suess effect) until the 1950s when that signal was overwhelmed by the much larger spike from atmospheric nuclear weapons tests (Fig. 2). Since the latter dominates, the total change from both anthropogenic effects is often referred to as bomb radiocarbon. As an anthropogenic transient tracer, bomb radiocarbon complements CFC-11, CFC-12, and SF_6 because of its different atmospheric history and much longer air-sea equilibration time (Broecker and Peng, 1974). Observations of bomb radiocarbon have been used to constrain the global mean gas transfer velocity (Broecker and Peng, 1982; Sweeney et al., 2007); however, in recent decades, ocean radiocarbon changes have become more sensitive to interior transport and mixing, making it behave more like anthropogenic CO_2 (Graven

et al., 2012). Hence it is particularly relevant to use radiocarbon observations to evaluate ocean carbon-cycle models that aim to assess uptake of anthropogenic carbon as done during OCMIP (e.g. Orr et al., 2001).

Information from the stable carbon isotope ^{13}C also helps to constrain the anthropogenic perturbation in dissolved inorganic carbon by exploiting the Suess effect (Quay et al., 1992, 2003). Driven by the release of anthropogenic CO_2 produced from

5 agriculture, deforestation, and fossil-fuel combustion, the Suess effect has resulted in a continuing reduction of the ^{13}C/^{12}C ratio relative to that of the preindustrial atmosphere-ocean system. That ratio is reported relative to a standard as δ^{13}C, which is not corrected for fractionation, unlike Δ^{14}C. Fractionation occurs during gas exchange and photosynthesis, and δ^{13}C is also sensitive to respiration of organic material and ocean mixing. Ocean δ^{13}C observations have been used to test marine ecosystem models, including processes such as phytoplankton growth rate, iron limitation, and grazing (Schmittner et al., 2013; Tagliabue

10 and Bopp, 2008) and may also provide insight into climate-related ecosystem changes. Past changes in δ^{13}C recorded in ice cores and marine sediments are likewise useful to evaluate models (Schmitt et al., 2012; Oliver et al., 2010).

Besides the aforementioned tracers to evaluate modeled circulation fields, OMIP-BGC also includes other passive tracers to compare simulated ocean biogeochemistry with data and among models, e.g. in terms of mean states, trends, and variability. Whereas all OCMIP2 groups used a common biogeochemical model (Najjar and Orr, 1998, 1999; Najjar et al., 2007), essen-

15 tially testing its sensitivity to different circulation fields, OMIP will not adopt the same approach. Rather, OMIP focuses on evaluating and comparing preselected ~~'combined'~~ "combined" ocean models (circulation-ice-biogeochemistry) largely defined already by individual groups planning to participate in CMIP6. Those combined ocean models will be evaluated when forced by reanalysis data as well as when coupled within the CMIP6 Earth System Models.

OMIP-BGC model groups will use common physical forcing for ocean-only models and common formulations for carbonate

20 chemistry, gas exchange, gas solubilities, and Schmidt numbers. ~~All~~ Biogeochemical models will be coupled ~~online with~~ to the ocean-ice ~~physics and~~ physical models, online (active and passive tracers will be modeled simultaneously), and they will be forced with the same atmospheric gas histories. Yet beyond those commonalities, model groups are free to choose their preferred ocean model configuration. For instance, groups may choose whether or not to include direct coupling between simulated chlorophyll and ocean dynamics. When coupled, chlorophyll is not a typical passive tracer; it is active in the sense

25 that it affects ocean circulation. Likewise, OMIP groups are free to use their preferred boundary conditions for the different sources of nutrients and micronutrients to the ocean via atmospheric deposition, sediment mobilization, and hydrothermal sources (e.g. for Fe) as well as lateral input of carbon from river and groundwater discharge. Biogeochemical models with riverine delivery of carbon and nutrients to the ocean usually include sediment deposition as well as loss of carbon from rivers back to the atmosphere through the air-sea exchange. Each group is free to use their preferred approach as long as mass is

30 approximately conserved. Groups are requested to provide global integrals of these boundary conditions and to document their approach, preferably in a peer-reviewed publication.

~~Thus~~ OMIP-BGC ~~has two initial goals:~~ aims to provide the technical foundation to assess trends, variability, and related uncertainties in ocean carbon and related biogeochemical variables since the onset of the industrial era and into the future. That foundation includes (1) ~~to provide~~ the OMIP-BGC protocols for groups that will include inert chemical tracers and biogeo-

35 chemistry in OMIP's two forced global ocean model simulations, which couple circulation, sea-ice, and biogeochemistry, and

(2) ~~to provide a~~ the complete list of ocean biogeochemical diagnostics for OMIP, but also for CMIP6 (Eyring et al., 2016) and any ocean-related MIPs under its umbrella, e.g. C4MIP (Jones et al., 2016).

Simulated results from OMIP-BGC will be exploited to contribute to OMIP's effort to study basic CMIP6 science questions on the origins and consequences of systematic model biases. In particular, OMIP-BGC offers a forum for ocean biogeochemical modelers and a technical framework by which they will assess and improve biases of simulated tracer and biogeochemical components of CMIP6's earth system models. ~~Among~~ OMIP-BGC will contribute to the World Climate Research Programme's (WCRP) Grand Challenges ~~, OMIP-BGC will contribute to~~ by providing fundamental information ~~necessary~~ needed to improve near-term climate prediction and carbon feedbacks in the climate system. Assessments will focus on current and future changes in ocean carbon uptake and storage, acidification, deoxygenation, and changes in marine productivity.

Novel analyses are expected from OMIP, in part because of recent improvements in the physical and biogeochemical components. For example, some of the physical models will have sufficient resolution to partially resolve mesoscale eddies. When coupled to biogeochemical models, that combination should allow OMIP to provide a first assessment of how air-sea CO_2 fluxes and related biogeochemical variables are affected by the ocean's intrinsic variability (also known as internal, chaotic, or unforced variability). Previous studies of the ocean's internal variability have focused only on physical variables (Penduff et al., 2011) . Other studies have assessed internal variablility of ocean biogeochemistry, but they account only for the component associated with turbulence in the atmosphere, i.e., they use a coarse-resolution ocean model coupled within an Earth System Model framework (Lovenduski et al., 2016) . Whether internal variablity from the ocean works to enhance or reduce that from the atmosphere will depend on the variable studied, the region, and the model. OMIP aims to provide a new insight on the ocean's contribution to internal variability while also quantifying the relative importance of the contribution of internal variability to overall uncertainty of model projections.

2 Protocols

As described by Griffies et al. (2016), the OMIP-Physics simulations consist of forcing physical model systems (an ocean general circulation model coupled to a sea-ice model) with the interannually varying atmospheric data reanalysis known as the Coordinated Ocean-ice Reference Experiments (CORE-II) available over 1948 to 2009 (Large and Yeager, 2009). For OMIP, that 62-yr forcing will be repeated five times to make simulations of 310 yr. OMIP-BGC participants will make these simulations by coupling their prognostic models of ocean biogeochemistry, online, to their physical model systems. These OMIP-BGC simulations will be forced by observed records of atmospheric CO_2 and other gases during the 310-yr period, defined as equivalent to calendar years 1700 to 2009. One 310-yr OMIP simulation *(omip1)*, with models initialized by data, is required (Tier 1) for all OMIP modeling groups; another 310-yr simulation *(omip1-spunup)*, with models initialized from a previous long spin-up simulation, is only for OMIP-BGC groups. Although optional, the *omip1-spunup* simulation is strongly encouraged (Tier 2) to minimize drift, assess deep-ocean ventilation, and separate physical vs. biological components of ocean carbon. Details of these simulations are provided below.

The two forced ocean model simulations, *omip1* and *omip1-spunup* differ from but are connected to the CMIP6 DECK and historical simulations. The only differences are the intialization and the forcing. In *omip1*, the ocean model is initialilzed with observations and forced by reanalysis data; in *historical* the ocean model is coupled within an Earth System Model Framework after some type of spin up. Likewise, the early portion of the *omip1-spunup* forced simulation is comparable to the CMIP6
5 DECK *piControl* coupled simulation. The complementarity of approaches will lead to a more thorough model evaluation.

When modeling chemical and biogeochemical tracers, it is recommended that OMIP groups use the same formulations for gas exchange and carbonate chemistry as outlined below. Little effort would be needed to modify code that is already consistent with previous phases of OCMIP. For gas exchange, model groups only need to change the value of the gas transfer coefficient, the formulations and coefficients for Schmidt numbers, and the atmospheric gas histories. For carbonate chemistry, groups
10 should strive to use the constants recommended for best practices (Dickson et al., 2007) on the total pH scale and to avoid common modeling assumptions that lead to significant biases, notably an oversimplified alkalinity equation (Orr and Epitalon, 2015). Fortran 95 code to make these calculations will be made available to OMIP-BGC participants.

2.1 Passive Tracers

2.1.1 Inert chemistry

15 The inert chemistry component of OMIP includes online simulation of CFC-11, CFC-12, and SF_6. While CFC-12 is required (~~level=~~priority 1), CFC-11 and SF_6 are encouraged (~~level=~~priority 2). About the same amount of observational data in the global ocean exists for both CFC-11 and CFC-12, starting with early field programs in the 1980s. But CFC-12 has a longer atmospheric history, with its production starting a decade earlier ($\sim$1936) and a slower decline starting a decade later due to its longer atmospheric lifetime (112 vs. 52 yr) relative to CFC-11 (Rigby et al., 2013). In contrast, SF_6 has continued to increase
20 rapidly in recent decades. That increase will continue for many years despite ongoing efforts to restrict production and release of this potent greenhouse gas, because SF_6's atmospheric lifetime is perhaps 3000 yr (Montzka et al., 2003). Using pairs of these tracers offers a powerful means to constrain ventilation ages; if model groups are only able to model two of these tracers, the ideal combination is CFC-12 and SF_6.

Simulation protocols are based on the OCMIP2 design document (Najjar and Orr, 1998) and its ensuing CFC protocol (Orr
25 et al., 1999a) and model comparison (Dutay et al., 2002). These inert passive tracers are computed online along with the active tracers (i.e. temperature and salinity in the physical simulation); they are independent of the biogeochemical model. OMIP models will be forced to follow historical atmospheric concentrations of CFC-11, CFC-12, and SF_6, accounting for gas exchange and their different solubilities and Schmidt numbers. The same passive tracers should be included in the forced OMIP simulations and in the coupled CMIP6 historical simulations. Both types of simulations will be analyzed within the framework
30 of OMIP. These inert chemistry tracers are complementary to the ideal age tracer that is included in the OMIP-Physics protocols (Griffies et al., 2016).

2.1.2 Biogeochemistry

For the other passive tracers, referred to as biogeochemistry, the OMIP-BGC protocols build on those developed for OCMIP. These include the OCMIP2 abiotic and biotic protocols (Najjar and Orr, 1998, 1999; Orr et al., 1999b) and the OCMIP3 protocols for interannually forced simulations (Aumont et al., 2004). Each model group will implement the OMIP protocol in their own prognostic ocean biogeochemical model as in OCMIP3, unlike the common-model approach of OCMIP2. Each OMIP biogeochemical model will be coupled online to an ocean general circulation model, forced by the CORE-II atmospheric state. Geochemical boundary conditions for the atmosphere include an imposed constant atmospheric concentration of O_2 (mole fraction x_{O_2} of 0.20946) but a variable atmospheric CO_2 that follows observations (Meinshausen et al., 2016).

In addition, OMIP-BGC simulations ~~will require~~ should include a natural carbon tracer that sees a constant atmospheric mole fraction of CO_2 in dry air (x_{CO_2}) fixed at the 1 January 1850 value (284.65 ppm), the CMIP6 preindustrial reference. This can be done either in an independent simulation with identical initial conditions and forcing, except for atmospheric x_{CO_2}, or in the same simulation by adding one or more new tracers to the biogeochemical model, referred to here as a *dual-C_T* simulation. For this *dual* simulation, OMIP modelers would need to add a second dissolved inorganic carbon tracer (C_T^{nat}), e.g. as in Yool et al. (2010). In OMIP, this added tracer will isolate natural CO_2 and keep track of model drift. Such *doubling* may also be necessary for other biogeochemical model tracers if they are directly affected by the CO_2 increase. For instance, expansion of the PISCES model (Aumont and Bopp, 2006) to a *dual-C_T* implementation resulted in doubling not only C_T but also its transported $CaCO_3$ tracer, which in turn affects total alkalinity A_T (Dufour et al., 2013). These natural tracers are referred to as C_T^{nat}, $CaCO_3^{nat}$, and A_T^{nat}. Calculated variables affected by CO_2 should also be doubled, including pH, pCO_2, the air-sea CO_2 flux, and carbonate ion concentration. If biology depends on CO_2, additional tracers such as nutrients and O_2 would also need to be doubled, making the doubling strategy less appealing. That strategy may also be more complex in some Earth System Models, e.g. if A_T changes abiotically due to warming-related changes in weathering and river runoff.

2.1.3 Abiotic carbon and radiocarbon

In the *omip1-spunup* simulation (as well as in its previously run spin up) OMIP-BGC groups will also include two abiotic tracers to simulate total dissolved inorganic carbon C_T^{abio} and corresponding radiocarbon $^{14}C_T^{abio}$. These abiotic tracers do not depend on any biotic tracers. They should be included in addition to the biotic carbon tracers mentioned above (C_T and C_T^{nat}). The ratio of the two abiotic tracers will be used to evaluate and compare models in terms of deep-ocean ventilation ages (natural radiocarbon) and near-surface anthropogenic invasion of bomb radiocarbon. In addition, C_T^{abio} will be compared to C_T to distinguish physical from biogeochemical effects on total carbon. For simplicity, simulations will be made abiotically following OCMIP2 protocols (Orr et al., 1999b). We recommend that participating groups add these two independent tracers to their biogeochemical model to simulate them simultaneously, thus promoting internal consistency while reducing costs.

In OMIP, we will use this two-tracer approach rather than the simpler approach of modeling only the $^{14}C/C$ ratio directly (Toggweiler et al., 1989a, b). That simpler approach would be a better choice if our focus were only on comparing simulated and field-based estimates of the ocean's bomb-^{14}C inventory, both of which are biased low (Naegler, 2009; Mouchet, 2013).

The simpler modeling approach underestimates the inventory, because it assumes a constant air-sea CO_2 disequilibrium during the industrial era; likewise, field reconstructions of the ocean's bomb-^{14}C inventory (Key et al., 2004; Peacock, 2004; Sweeney et al., 2007) are biased low because they assume that ocean C_T is unaffected by the anthropogenic perturbation. Yet in terms of oceanic Δ^{14}C, the simple and the two-tracer approaches yield similar results (Mouchet, 2013), because the effect of increasing C_T on oceanic Δ^{14}C is negligible (Naegler, 2009). We also choose the two-tracer approach to take advantage of its C_T^{abio} tracer to help distinguish physical from biological contributions to C_T.

To model ^{14}C, OMIP neglects effects due to fractionation (i.e. from biology and gas exchange). Hence model results will be directly comparable to measurements reported as Δ^{14}C, a transformation of the ^{14}C/C ratio designed to correct for fractionation (Toggweiler et al., 1989a). Thus biases associated with our abiotic approach may generally be neglected. For natural ^{14}C, Bacastow and Maier-Reimer (1990) found essentially identical results for simulations that accounted for biological fractionation vs. those that did not, as long as the atmospheric CO_2 boundary conditions were identical. For bomb ^{14}C, which also includes the Suess effect, neglecting biological fractionation results in small biases (Joos et al., 1997).

Hence for the *omip1-spunup* simulation, OMIP-BGC groups will simulate four flavors of dissolved inorganic carbon: biotic natural (C_T^{nat}), biotic total (C_T), abiotic total (C_T^{abio}), and abiotic radiocarbon ($^{14}C_T^{abio}$). Conversely for the *omip1* simulation, groups will simulate only the first two flavors, C_T^{nat} and C_T. These tracers may be simulated simultaneously or in separate simulations, although we recommend the former.

2.1.4 Carbon-13

Groups that have experience modeling ^{13}C in their biogeochemical model are requested to include it as a tracer in the OMIP-BGC simulations. Groups without experience should avoid adding it. It is not required to simulate ^{13}C in order to participate in OMIP. Modeling groups that will simulate ocean ^{13}C are requested to report net air-sea fluxes of $^{13}CO_2$ and concentrations of total dissolved inorganic carbon-13 ($^{13}C_T$) for the *omip1-spunup* simulation. In Sect. 2.5 we recommend how isotopic fractionation during gas exchange should be modeled. Carbon-13 is typically included in ocean models as a biotic variable influenced by fractionation effects during photosynthesis that depend on growth rate and phytoplankton type. Some; some models also include fractionation during calcium carbonate formation (e.g., Tagliabue and Bopp, 2008) . Modeling groups should incorporate ecosystem fractionation specific to their ecosystem model formulation. We do not request modeling groups to report variables related to ^{13}C in phytoplankton or other organic carbon pools, only $^{13}C_T$ and net air-sea $^{13}CO_2$ fluxes.

2.2 Duration and initialization

As described by (Griffies et al., 2016), the physical components of the models are to be forced over 310 years, i.e. over five repeated forcing cycles of the 62-year CORE-II forcing (1948–2009). The biogeochemistry should be included, along with the physical system, during the full 310 years (1700–2009) and the inert chemistry only during the last 74 years (1936–2009). The biogeochemical simulations will be initialized on calendar date 01 January 1700, at the start of the first CORE-II forcing cycle.

The inert anthropogenic chemical tracers (CFC-11, CFC-12, SF_6) will be initialized to zero on 01 January 1936, during the fourth CORE-II forcing cycle at model date 01 January 0237.

For the *omip1* simulation, biogeochemical tracers will be initialized generally with observational climatologies. Fields from the 2013 World Ocean Atlas (WOA2013) will be used to initialize model fields of oxygen (Garcia et al., 2014a) as well as nitrate, total dissolved inorganic phosphorus, and total dissolved inorganic silicon (Garcia et al., 2014b). The latter two nutrients are often referred to simply as phosphate and silicate, but other inorganic P and Si species also contribute substantially to each total concentration (Fig. 3). Indeed it is the total dissolved concentrations (P_T and Si_T) that are both modeled and measured. OMIP will provide all these initial biogeochemical fields by merging WOA2013's means for January, available down to 500 m (for nitrate, phosphate and silicate), and down to 1500m for oxygen, with its annual mean fields below.

Model fields for A_T and preindustrial C_T will be initialized with gridded data from version 2 of the Global Ocean Data Analysis Project (GLODAPv2) from Lauvset et al. (2016), based on discrete measurements during WOCE and CLIVAR (Olsen et al., 2016). For greater consistency with GLODAPv1, OMIP-BGC model groups will use the C_T and A_T fields from GLODAPv2's first period (1986–1999, the WOCE era). To initialize modeled dissolved organic carbon (DOC), OMIP provides fields from the adjoint model from Schlitzer (Hansell et al., 2009). For dissolved iron (Fe), OMIP simulations will not be initialized from observations because a full-depth, global 3-D data climatology is unavailable due to lack of data coverage, particularly in the deep ocean. Hence for initial Fe fields, OMIP provides the median model result from the Iron Model Intercomparison Project (FeMIP, Tagliabue et al., 2016). Yet that initialization field may not be well suited for all Fe models, which differ greatly. Although OMIP provides initialization fields for Fe and DOC, their actual initialization is left to the discretion of each modeling group. In a previous comparison (Kwiatkowski et al., 2014), groups did not initialize modeled Fe with a common field nor approach because the complexity of the Fe cycle differed greatly among models. Likewise, there was no common approach to initialize DOC because biogeochemical models vary greatly in the way they represent its lability. Initialization of other tracers is less critical, e.g. phytoplankton biomass is restricted to the top 200 m and equilibrates rapidly as do other biological tracers.

The *omip1* simulation is relatively short and is thus manageable by all groups, but many of its tracers will have large drifts because model initial states will be far from their equilibrium states. These drifts complicate assessment of model performance based on model-data agreement (Séférian et al., 2015). Hence a complementary simulation, *omip1-spunup*, is proposed, where biogeochemical tracers are initialized instead with a near-equilibrium state. Model groups may generate this spun-up initial state by any means at their disposal. The classic approach would be to spin up the model. That could be done either online, repeating many times the same physical atmospheric forcing (CORE-II), or offline, repeatedly cycling the physical transport fields from a circulation model forced by a single loop of the CORE-II forcing. If possible, the spin-up should be run until it reaches the equilibrium criteria adopted for OCMIP2. These criteria state that the globally integrated, biotic and abiotic air-sea CO_2 fluxes (F_{CO_2} and $F_{CO_2}^{abio}$) should each drift by less than $0.01 \, \mathrm{Pg \, C \, yr^{-1}}$ (Najjar and Orr, 1999; Orr et al., 1999b) and that abiotic $^{14}C_T$ should be stabilized to the point that 98% of the ocean volume has a drift of less than $0.001 \, \%_0 \, \mathrm{yr^{-1}}$ (Aumont et al., 1998). The latter is equivalent to a drift of about 10 yr in the ^{14}C age per 1000 yr of simulation. For most models, these drift criteria can be reached only after integrations of a few thousand model years. To reach the spun-up state with the classic

approach, we request that groups spin up their model for at least 2000 yr, if at all possible. Other approaches to obtain the spun-up state, such as using tracer-acceleration techniques or fast solvers (Li and Primeau, 2008; Khatiwala, 2008; Merlis and Khatiwala, 2008) are also permissible. If used, they should also be applied until models meet the same equilibrium criteria described above.

5   The spin-up simulation itself should be initialized as for the *omip1* simulation, except for the abiotic tracers and the $^{13}C_T$ tracer. The abiotic initial fields of A_T^{abio} and C_T^{abio} will be provided, being derived from initial fields of T and S. Although C_T^{abio} is a passive tracer carried in the model, A_T^{abio} is not. The latter will be calculated from the initial 3-D salinity field as detailed below; then that calculated field will be used to compute C_T^{abio} throughout the water column assuming equilibrium with the preindustrial level of atmospheric CO_2 at the initial T and S conditions (using OMIP's carbonate chemistry routines).

10   For $^{14}C_T^{\mathrm{abio}}$, initial fields will be based on those from GLODAPv1 for natural $\Delta^{14}C$ (Key et al., 2004). OMIP will provide these fields with missing grid <cells filled based on values from adjacent ocean grid points. Groups that include $^{13}C_T$ in *omip1-spunup* should initialize that in the precursor spin-up simulation to 0‰ following the approach of Jahn et al. (2015). Beware though that equilibration timescales for ^{13}C are longer than for C_T, implying the need for a much longer spin up.

2.3   Geochemical atmospheric forcing

15   The atmospheric concentration histories of the three inert chemical tracers (CFC-11, CFC-12, and SF_6) to be used in OMIP are summarized by Bullister (2015) and shown in Fig. 1. Their atmospheric values are to be held to zero for the first three cycles of the CORE-II forcing, then increased starting on 01 January 1936 (beginning of model year 0237) according to the OMIP protocol. To save computational resources, the inert chemical tracers may be activated only from 1936 onward, starting from zero concentrations in the atmosphere and ocean. The atmospheric CO_2 history used to force the OMIP models is the same as that used for the CMIP6 historical simulation (Meinshausen et al., 2016), while carbon isotope ratios ($\Delta^{14}C$ and $\delta^{13}C$) are the same as those used by C4MIP (Jones et al., 2016). These atmospheric records of CO_2 and carbon isotope ratios (Fig. 2) and those for the inert chemical tracers will be made available on the CMIP6 web site. The biogeochemical tracers are to be activated at the beginning of the 310-year simulation (on 01 January 1700), but initialized differently as described above for *omip1* and *omip1-spunup*. The atmospheric concentration of CO_2 is to be maintained at the CMIP6 preindustrial reference of $xCO_2^{\mathrm{atm}} = 284.65$ ppm between calendar years 1700.0 and 1850.0, after which it must increase following observations (Meinshausen et al., 2016). The increasing xCO_2^{atm} will thus affect C_T but not C_T^{nat}, which sees only the preindustrial reference level of xCO_2^{atm}. The increasing xCO_2^{atm} is also seen by $^{13}C_T$ and the two abiotic tracers, C_T^{abio} and $^{14}C_T^{\mathrm{abio}}$, to be modeled only in the *omip1-spunup* simulation and its spin up.

2.4   Conservation equation

30   The time evolution equation for all passive tracers is given by

$$\frac{\partial C}{\partial t} = \mathbf{L}(C) + J_C,$$ (1)

where C is the tracer concentration; $\mathbf{L}$ is the 3-D transport operator, which represents effects due to advection, diffusion, and convection; and J_C is the internal source-sink term. Conservation of volume is assumed in Eq. 1 and standard units of $mol\,m^{-3}$ are used for all tracers. For the inert chemical tracers (CFC-11, CFC-12, and SF_6), $J_C = 0$. For the abiotic carbon tracers, in the *omip1-spunup* simulation and its spin up, the same term is also null for the total carbon tracer C_T

$$J_{C_T^{abio}} = 0, \tag{2}$$

but not for the total radiocarbon tracer $^{14}C_T^{abio}$ due to radioactive decay

$$J_{^{14}C_T^{abio}} = -\lambda\,^{14}C_T^{abio}, \tag{3}$$

where λ is the radioactive decay constant for ^{14}C, i.e.

$$\lambda = ln(2)/5700\,yr = 1.2160 \times 10^{-4}\,yr^{-1}, \tag{4}$$

converted to s^{-1} using the number of seconds per year in a given model. For other biogeochemical tracers J_C is non-zero and often differs between models. For $^{13}C_T$, J_C includes isotopic fractionation effects.

2.5 Air-sea gas exchange

Non-zero surface boundary conditions must also be included for all tracers that are affected by air-sea gas exchange: CFC-11, CFC-12, SF_6, dissolved O_2, and dissolved inorganic carbon in its various modeled forms (C_T, C_T^{nat}, C_T^{abio}, $^{14}C_T^{abio}$, and $^{13}C_T$). In OCMIP2, surface boundary conditions also included a virtual-flux term for some biogeochemical tracers, namely in models that had a virtual salt flux because they did not allow water transfer across the air-sea interface. Water transfer calls for different implementations depending on the way the free-surface is treated, as discussed extensively by Roullet and Madec (2000). Groups that have implemented virtual fluxes for active tracers (T and S) should follow the same practices to deal with virtual fluxes of passive tracers such as C_T and A_T, as detailed in the OCMIP2 design document (Najjar and Orr, 1998) and in the OCMIP2 Abiotic HOWTO (Orr et al., 1999b). In OMIP, all models should report air-sea CO_2 fluxes due to gas exchange (F_{CO_2}, $F_{CO_2}^{nat}$, $F_{CO_2}^{abio}$, $F_{^{14}CO_2}^{abio}$, and $F_{^{13}CO_2}$) without virtual fluxes included. Virtual fluxes are not requested as they do not directly represent CO_2 exchange between the atmosphere and ocean.

Surface boundary fluxes may be coded simply as adding source-sink terms to the surface layer, e.g.

$$J_A = \frac{F_A}{\Delta z_1}, \tag{5}$$

where for gas A, J_A is its surface-layer source-sink term due to gas exchange ($mol\,m^{-3}\,s^{-1}$) and F_A is its air-to-sea flux ($mol\,m^{-2}\,s^{-1}$), while Δz_1 is the surface-layer thickness (m).

In OMIP, we parameterize air-sea gas transfer of CFC-11, CFC-12, SF_6, O_2, CO_2, $^{14}CO_2$, and $^{13}CO_2$ using the gas transfer formulation also adopted for OCMIP2 (excluding effects of bubbles):

$$F_A = k_w \left([A]_{sat} - [A]\right), \tag{6}$$

where for gas A, k_w is its gas transfer velocity, $[A]$ is its simulated surface-ocean dissolved concentration, and $[A]_{sat}$ is its corresponding saturation concentration in equilibrium with the water-vapor-saturated atmosphere at a total atmospheric pressure P_a. Concentrations throughout are indicated by square brackets and are in units of mol m^{-3}.

For all gases that remain purely in dissolved form in seawater, gas exchange is modeled directly with Eq. (6). However for C_T, only a small part remains as dissolved gas as mentioned in Sect. 2.6. Thus the dissolved gas concentration $[CO_2^*]$ must first be computed, each time step, from modeled C_T and A_T and then the gas exchange is computed with Eq. (6). For example, for the two abiotic tracers (in *omip1-spunup*):

$$F_{CO_2}^{abio} = k_w \left([CO_2^*]_{sat} - [CO_2^*] \right) \tag{7}$$

and

$$F_{^{14}CO_2}^{abio} = k_w \left(\left[^{14}CO_2^* \right]_{sat} - \left[^{14}CO_2^* \right] \right). \tag{8}$$

For ^{13}C, isotopic fractionation associated with gas exchange must be included in the flux calculation. We recommend using the formulation of Zhang et al. (1995)

$$F_{^{13}CO_2} = k_w \, \alpha_k \, \alpha_{aq-g} \left(^{13}R_{\text{atm}} \, [CO_2^*]_{\text{sat}} - \frac{\left[^{13}CO_2^* \right]}{\alpha_{C_T-g}} \right), \tag{9}$$

where α_k is the kinetic fractionation factor, α_{aq-g} is the fractionation factor for gas dissolution, and α_{C_T-g} is the equilibrium fractionation factor between dissolved inorganic carbon and gaseous CO_2. $^{13}R_{\text{atm}}$ is the ^{13}C/^{12}C ratio in atmospheric CO_2. Following Zhang et al. (1995), α_{C_T-g} depends on T and the fraction of carbonate in C_T, fCO$_3$:

$$\alpha_{C_T-g} = \frac{0.0144 \, T_c \, fCO_3 - 0.107 \, T_c + 10.53}{1000} + 1, \tag{10}$$

where T_c is temperature in units of $^\circ$C, while division by 1000 and addition of 1 converts the fractionation factor from ϵ in units of ‰ into α. The α_{aq-g} term depends on temperature following

$$\alpha_{aq-g} = \frac{0.0049 \, T_c - 1.31}{1000} + 1. \tag{11}$$

Conversely no temperature dependence was found for α_k. Hence we recommend that OMIP modelers use a constant value for α_k of 0.99914 (ϵ_k of -0.86‰), the average from Zhang et al.'s measurements at 5° and 21°C.

2.5.1 Gas transfer velocity

OMIP modelers should use the instantaneous gas transfer velocity k_w parameterization from Wanninkhof (1992), a quadratic function of the 10-m wind speed u

$$k_W = a \left(\frac{Sc}{660} \right)^{-1/2} u^2 \left(1 - f_i \right), \tag{12}$$

to which we have added limitation from sea-ice cover following OCMIP2. Here a is a constant, Sc is the Schmidt number, and f_i is the sea-ice fractional coverage of each grid cell (varying from 0 to 1). Normally, the constant a is adjusted so that

wind speeds used to force the model are consistent with the observed global inventory of bomb ^{14}C, e.g. as done in previous phases of OCMIP (Orr et al., 2001; Najjar et al., 2007). Here though, we choose to use one value of a for all simulations, independent of whether models are used in forced (OMIP) or coupled mode (i.e. in CMIP6 DECK [Diagnostic, Evaluation and Characterization of Klima] and historical simulations). For a in OMIP, we rely on the reassessment from Wanninkhof (2014) who used improved estimates of the global-ocean bomb-^{14}C inventory along with CCMP (Cross Calibrated Multi-Platform) wind fields in an inverse approach with the Modular Ocean Model (Sweeney et al., 2007) to derive a best value of

$$a = 0.251 \, \frac{\text{cm}\,\text{hr}^{-1}}{(\text{m}\,\text{s}^{-1})^2}, \tag{13}$$

which will give k_w is in cm hr^{-1} if winds speeds are in m s^{-1}. For model simulations where tracers are carried in mol m^{-3}, k_w should be in units of m s^{-1}; thus, a should be set equal to 6.97×10^{-7} m s^{-1}. The same value of a should be adopted for the forced OMIP simulations and for Earth System Model simulations made under CMIP6.

2.5.2 Schmidt number

Besides a, the Schmidt number Sc is also needed to compute the gas transfer velocity (Eq. 12). The Schmidt number is the ratio of the kinematic viscosity of water μ to the diffusion coefficient of the gas D ($Sc = \mu/D$). The coefficients for the fourth-order ~~polynomical~~ polynomial fit of Sc to *in situ* temperature over the temperature range of -2 to $40°$C (Wanninkhof, 2014) are provided in Table 1 for each gas to be modeled in OMIP and CMIP6. Fortran 95 routines using the same formula and coefficients for all gases modeled in OMIP are available for download via the *gasx* module of the *mocsy* package (Sect. 2.6).

2.5.3 Atmospheric saturation concentration

The surface gas concentration in equilibrium with the atmosphere (saturation concentration) is

$$[A]_{sat} = K_0 \, f_A = K_0 \, C_f \, p_A = K_0 \, C_f \, (P_a - p\text{H}_2\text{O}) \, x_A, \tag{14}$$

where for gas A, K_0 is its solubility, f_A is its atmospheric fugacity, C_f is its fugacity coefficient, p_A is its atmospheric partial pressure, and x_A is its mole fraction in dry air, while P_a is again the total atmospheric pressure (atm) and $p\text{H}_2\text{O}$ is the ~~water vapor pressure at saturation~~ vapor pressure of water (also in atm) at sea surface temperature and salinity (Weiss and Price, 1980).

The combined term $K_0 \, C_f \, (P_a - p\text{H}_2\text{O})$ is available at $P_a = 1$ atm (i.e. P_a^0) for all modeled gases except oxygen. We denote this combined term as ϕ_A^0 (at P_a^0) ; elsewhere it is known as the solubility function F (e.g. Weiss and Price, 1980; Warner and Weiss, 1985; Bullister et al., 2002) but we do not use the latter notation here to avoid confusion with the air-sea flux (Eq. 6). For four of the gases to be modeled in OMIP, the combined solubility function ϕ_A^0 has been computed using the empirical fit

$$ln\left(\phi_A^0\right) = a_1 + a_2 \left(\frac{100}{T}\right) + a_3 \, ln\left(\frac{T}{100}\right) + a_4 \left(\frac{T}{100}\right)^2 + S\left[b_1 + b_2 \left(\frac{T}{100}\right) + b_3 \left(\frac{T}{100}\right)^2\right], \tag{15}$$

where T is the model's in-situ, absolute temperature (ITS90) and S is its salinity in permil (PSS-78). Thus separate sets of coefficients are available for CO_2 (Weiss and Price, 1980, Table VI), CFC-11 and CFC-12 (Warner and Weiss, 1985, Table 5),

13

and SF_6 (Bullister et al., 2002, Table 3), the values of which are detailed in Table 2. For O_2, it is not ϕ_A^0 that is available but rather $[O_2]_{sat}^0$ (Garcia and Gordon, 1992) as detailed below.

Both the solubility function ϕ_A^0 and the saturation concentration $[A]_{sat}^0$ can be used at any atmospheric pressure P_a, with errors of less than 0.1%, by approximating Eq. (14) as

5 $$[A]_{sat} = \frac{P_a}{P_a^0} \phi_A^0 \, x_A = \frac{P_a}{P_a^0} \, [A]_{sat}^0,$$ (16)

where P_a^0 is the reference atmospheric pressure (1 atm). Variations in surface atmospheric pressure must not be neglected in OMIP because they alter the regional distribution of $[A]_{sat}$. For example, the average surface atmospheric pressure between $60°$ and $30°$S is 3% lower than the global mean, thus reducing surface-ocean pCO_2 by $10\,\mu$atm and $[O_2]_{sat}$ by $10\,\mu$mol kg^{-1}. The atmospheric pressure fields used to compute gas saturations should also be consistent with the other physical forcing. Thus

10 for the OMIP forced simulations, modelers will use surface atmospheric pressure from CORE II, converted to atm.

For the two abiotic carbon tracers, abbreviating $K' = K_0 C_f$, we can write their surface saturation concentrations (Eq. 14) as

$$[CO_2^*]_{sat}^{abio} = K' \, (P_a - pH_2O) \, x_{CO_2}$$ (17)

and

15 $$\left[^{14}CO_2^*\right]_{sat}^{abio} = [CO_2^*]_{sat} \, ^{14}r'_{atm}.$$ (18)

Here $^{14}r'_{atm}$ represents the normalized atmospheric ratio of ^{14}C/C, i.e.

$$^{14}r'_{atm} = \frac{^{14}r_{atm}}{^{14}r_{std}} = \left(1 + \frac{\Delta^{14}C_{atm}}{1000}\right),$$ (19)

where $^{14}r_{atm}$ is the atmospheric ratio of ^{14}C/C, $^{14}r_{std}$ is the analogous ratio for the standard (1.170×10^{-12}, see Appendix A), and $\Delta^{14}C_{atm}$ is the atmospheric $\Delta^{14}C$, the fractionation-corrected ratio of $^{14}C/C$ relative to a standard reference given

20 in permil (see below). We define $^{14}r'_{atm}$ and use it in Eq. (18) to be able to compare C_T^{abio} and $^{14}C_T^{abio}$, directly, potentially simplifying code verification and testing. With the above model formulation for the OMIP equilibrium run (where $xCO_2^{atm} = 284.65$ ppm and $\Delta^{14}C^{atm} = 0$ ‰), both C_T^{abio} and $^{14}C_T^{abio}$ have identical units. Short tests with the same initialization for both tracers can thus verify consistency. Differences in the spin-up simulation will stem only from different initializations and radioactive decay. Differences will grow further during the anthropogenic perturbation (in *omip1-spunup*, i.e. after spin up),

25 because of the sharp contrast between the shape of the atmospheric histories of xCO_2 and $\Delta^{14}C_{atm}$.

For ^{13}C, the $\delta^{13}C_{atm}$ in atmospheric CO_2 is incorporated into Eq. (9) through the term $^{13}R_{atm}$, which is given by

$$^{13}R_{atm} = \left(\frac{\delta^{13}C_{atm}}{1000} + 1\right) \, ^{13}R_{std},$$ (20)

where $^{13}R_{std}$ is the standard ratio 0.0112372 (Craig, 1957). In this formulation, unlike for $^{14}C_T^{abio}$, $^{13}C_T$ is not normalized by the standard ratio. However, modeling groups may wish to simulate normalized $^{13}C_T$, e.g. by including a factor of $1/^{13}R_{std}$

analogous to the approach used for $^{13}C_T^{abio}$. Modeling groups that simulate ^{13}C in OMIP must report non-normalized values of the concentration $^{13}C_T$ and the air-sea flux $F_{^{13}CO_2}$. No other ^{13}C results are requested.

For all gases simulated in OMIP, the atmospheric saturation concentration $[A]_{sat}$ is computed using Eq. (16). For all gases except oxygen, the combined solubility function ϕ_A^0 is available, being computed each time step using modeled T and S with Eq. (15), the corresponding gas-specific coefficients (Table 2), and the atmospheric mole fraction of each gas x_A. The exception is O_2 because rather than x_A and ϕ_A^0, it is the reference saturation concentration $[O_2]_{sat}^0$ that is available (Garcia and Gordon, 1992, equation 8, Table 1).

In all cases, the same P_a/P_a^0 term is used to account for effects of atmospheric pressure (Eq. 16). For P_a, modelers must use the fields of surface atmospheric pressure *(sap)* from CORE II, i.e. for OMIP's forced ocean simulations (*omip1* and *omip1-spunup*), whereas for any CMIP6 coupled simulation, modelers should use *sap* from the coupled atmospheric model.

To compute $[A]_{sat}$ then, we only need one additional type of information, namely the x_A's for each of CO_2, CFC-11, CFC-12, and SF_6 as well as corresponding atmospheric histories for carbon isotopes:

1. x_{CFC-11}, x_{CFC-12}, and x_{SF_6}: Atmospheric records for observed CFC-11 and CFC-12 (in parts per trillion - ppt) are based on station data at 41°S and 45°N from (Walker et al., 2000) with subsequent extensions as compiled by Bullister (2015). For OMIP, each station will be treated as representative of its own hemisphere, except between 10°S and 10°N where those station values will be interpolated linearly as a function of latitude. Thus there are 3 zones: 90°S–10°S, where CFC's are held to same value as at the station at 41°S; 10°S–10°N, a buffer zone where values are interpolated linearly; and 10°N–90°N, where values are held to the same value as at the measuring station at 45°N. For SF_6, OMIP also relies on the Bullister (2015) synthesis over the same latitudinal bands. Values for all three inert chemical tracers are given at mid-year. It is recommended that modelers linearly interpolate these mid-year values to each time step, because annual growth rates can be large and variable.

2. x_{CO_2}: In the *spin-up* simulation, needed to initialize *omip1-spunup* simulation, atmospheric CO_2 is held constant at $x_{CO_2} = 284.65$ ppm, the same preindustrial value as used for the CMIP6 *picontrol* simulation. Over the industrial era, defined as between years 1850.0 and 2010.0 for both of OMIP's transient simulations (*omip1* and *omip1-spunup*), atmospheric x_{CO_2} will follow the same observed historical increase as provided for CMIP6 (Meinshausen et al., 2016). Modelers should use the record of global annual mean atmospheric x_{CO_2}, interpolated to each time step. That increasing x_{CO_2} affects the total tracer C_T in both transient simulations as well as the two abiotic tracers and $^{13}C_T$ in the *omip1-spunup* simulation. However, it does not affect the natural tracer C_T^{nat}, for which the atmosphere is always held at $x_{CO_2} = 284.65$ ppm.

3. $\Delta^{14}C^{atm}$: For the OMIP spin-up simulation, $\Delta^{14}C^{atm}$ is held constant at 0‰. For the *omip1-spunup* simulation, the equilibrium reference is thus year 1850.0. Then the model must be integrated until 2010.0 following the observed record of $\Delta^{14}C^{atm}$ (Levin et al., 2010), separated into three latitudinal bands (90°S–20°S, 20°S–20°N, and 20°N–90°N).

4. $\delta^{13}C^{atm}$: The atmospheric record of $\delta^{13}C$ is the same as adopted for C4MIP, a compilation of ice-core data (Rubino et al., 2013) and atmospheric measurements at Mauna Loa (Keeling, 2001).

2.5.4 Surface ocean concentration

The equation above for the atmospheric equilibrium (saturation) concentration of a gas (Eq. 14) should not be confused with the analogous equation for the simulated ocean concentration. The surface-ocean equation allows conversion between the simulated surface-ocean dissolved gas concentration $[A]$, the corresponding fugacity f_O, and the partial pressure p_O of the surface ocean as follows:

$$[A] = K_0\, f_O = K_0\, C_f\, p_O = K'\, p_O. \tag{21}$$

This surface-ocean equation is analogous to that for the atmospheric equilibrium saturation concentration $[A]_{sat}$ (Eq. 14), except that the ocean equation omits the final portion of the atmospheric equation which computes the mole fraction, a conventional parameter only for the atmosphere. Thus the combined term that includes the atmospheric pressure and humidity corrections (last term in parentheses) in Eq. (14) is not pertinent for the surface ocean equation. It should not be used when converting between simulated oceanic $[A]$ and the corresponding p_O. Confusion on this point was apparent in the publicly available OMIP2 code, i.e. for the conversion from $[CO_2^*]$ to pCO_2, although that did not affect simulated F_{CO_2}.

To avoid potential confusion and redundancy, OMIP modelers may prefer to separately compute the parts of ϕ_A rather than computing ϕ_A^0 and using it directly. Since

$$\phi_A = K_0\, C_f\, (P_a - pH_2O) = K'\, (P_a - pH_2O), \tag{22}$$

modelers need only compute K', and use that in both the ocean equation (Eq. 21) and the atmospheric saturation equation (Eq. 14), while for the latter also correct for atmospheric pressure and humidity, i.e. the $(P_a - pH_2O)$ term. That combined correction is to be computed with P_a from the CORE II forcing and with pH_2O calculated from model surface T and S (Weiss and Price, 1980, Eq. 10):

$$pH_2O = 24.4543 - 67.4509 \left(\frac{100}{T}\right) - 4.8489\, ln\left(\frac{T}{100}\right) - 0.000544\, S, \tag{23}$$

where pH_2O is in atm, T is the in-situ, absolute temperature and S is salinity in permil. In this way, OMIP modelers may avoid using the sometimes confusing combined term ϕ_A^0 altogether as well as its approximative pressure correction when calculating the saturation concentration (Eq. 16). Pressure corrections for K' may be neglected in the surface ocean where total pressure remains close to 1 atm (Weiss, 1974).

The ocean equation (Eq. 21) converts a simulated dissolved gas concentration to a partial pressure using its combined product K', which can be computed directly for some gases or via a two-step process for others. For OMIP's inert chemical tracers, tabulated coefficients can be used to compute K' directly, i.e. for CFC-11 and CFC-12 (Warner and Weiss, 1985, Table 2) and for SF_6 (Bullister et al., 2002, Table 2) using modeled T and S in an equation just like Eq. 15 but without the first T^2 term ($a_4 = 0$):

$$ln(K') = a_1 + a_2 \left(\frac{100}{T}\right) + a_3\, ln\left(\frac{T}{100}\right) + S\left[b_1 + b_2 \left(\frac{T}{100}\right) + b_3 \left(\frac{T}{100}\right)^2\right], \tag{24}$$

where T is the in-situ absolute temperature and S is salinity in permil.

For O_2, K' is not needed for the saturation calculations, but it is necessary when using the simulated dissolved $[O_2]$ to compute the corresponding surface ocean pO_2, a required variable for OMIP and CMIP6. That solubility conversion factor K' can be derived by substituting its definition into Eq. (14) and rearranging, so that

$$K'_{O2} = \frac{[O_2]^0_{sat}}{x_{O_2}(P_a^0 - p\mathrm{H_2O})},\tag{25}$$

where the numerator is from Eq. 8 of Garcia and Gordon (1992) using coefficients from their Table 1, and the denominator is the product of the corresponding constant atmospheric mole fraction of O_2 ($x_{O_2} = 0.20946$) and the wet-to-dry correction at 1 atm as described above. The computed K'_{O2} is then exploited to compute the partial pressure of oxygen ($pO_2 = [O_2]/K'_{O2}$).

For CO_2, tabulated coefficients are not available to compute K', but they are available to compute K_0 (Weiss, 1974, Table 1). Hence given that $K' = K_0 C_f$, modelers must also compute the fugacity coefficient C_f from Eq. 9 of Weiss (1974):

$$C_f = \exp\left[\left(B + 2x_2^2\,\delta_{12}\right)\frac{P_{\mathrm{ao}}}{RT}\right],\tag{26}$$

where B is the virial coefficient of CO_2 (Weiss, 1974, Eq. 6), x_2 is the sum of the mole fractions of all remaining gases ($1 - x\mathrm{CO_2}$, when $x\mathrm{CO_2} \ll 1$), and $\delta_{12} = 57.7 - 0.118T$. Here P_{ao} is the total pressure (atmospheric + hydrostatic) in atm, R is the gas constant ($82.05736\,\mathrm{cm^3\,atm\,mol^{-1}\,K^{-1}}$), and T is the in-situ absolute temperature (K).

Although the surface ocean concentration of dissolved carbon dioxide gas $[CO_2^*]$ is needed to compute air-sea CO_2 exchange, it is not that inorganic carbon species that is carried as a tracer in ocean carbon models (Sect. 2.6). Instead the $[CO_2^*]$ concentration ($\mathrm{mol\,m^{-3}}$) must be computed each time step from a model's simulated surface C_T, A_T, T, and S as well as nutrient concentrations (total dissolved inorganic phosphorus P_T and silicon Si_T) as detailed in the following section. All OMIP biogeochemical models will carry C_T and A_T as passive tracers. Most if not all will also carry at least one inorganic nutrient, nitrogen or phosphorus. Some will carry silicon. For models that carry only nitrogen, it is preferred that they compute P_T by dividing the total dissolved inorganic nitrogen concentration by 16, the constant N:P ratio from Redfield et al. (1963). For models without Si_T, it is preferred that they use climatological Si_T data interpolated to their model grid (i.e. annual average data from WOA2013). These options offer a better alternative than assuming nutrient concentrations are zero, which lead to systematic shifts of order of 10 μatm in calculated surface-water pCO_2.

The abiotic portion of the biogeochemical simulation, carries only two tracers, C_T^{abio} and $^{14}C_T^{abio}$, which are not connected to other biogeochemical tracers. Hence to compute corresponding abiotic $[CO_2^*]$ and $\left[^{14}CO_2^*\right]$ concentrations, we also need abiotic alkalinity. Following OCMIP2, the abiotic alkalinity in OMIP will be calculated simply as a normalized linear function of salinity:

$$A_T^{abio} = \overline{A_T} * \frac{S}{\overline{S}},\tag{27}$$

where $\overline{A_T}$ is the global mean of surface observations 2297 $\mu\mathrm{mol\,kg^{-1}}$ (Lauvset et al., 2016) and $\overline{S}$ is the model's global- and annual-mean surface salinity. In practice, it is recommended that $\overline{S}$ is first computed as the global mean of the initial salinity field and then, after one year of simulation, from the annual mean salinity of the previous year. Also needed are two other

input arguments, P_T and Si_T. Although accounting for both of their acid systems makes a difference, these abiotic tracers are not included along with abiotic C_T. Hence we take their concentrations as being constant, equal to the global mean of surface observations for P_T of 0.5 $\mu\text{mol kg}^{-1}$ and for Si_T of 7.5 $\mu\text{mol kg}^{-1}$. The assumption of constant nutrient distributions applies only to the carbonate chemistry calculations for abiotic C_T.

5   For the abiotic simulation's radiocarbon tracer, we must likewise compute its surface-ocean dissolved gas concentration $\left[^{14}\text{CO}_2^*\right]$. The latter is related to the calculated dissolved gas concentration of the stable abiotic carbon tracer as follows:

$$\left[^{14}\text{CO}_2^*\right]^{\text{abio}} = [\text{CO}_2^*]^{\text{abio}}\ {}^{14}r'_{\text{ocn}}, \tag{28}$$

where

$$^{14}r'_{\text{ocn}} = \frac{{}^{14}r_{\text{ocn}}}{{}^{14}r_{\text{std}}} = \frac{{}^{14}C_T^{\text{abio}}}{C_T^{\text{abio}}} \tag{29}$$

10   and $^{14}r_{\text{ocn}}$ is the $^{14}\text{C/C}$ of seawater. This normalization essentially means that $^{14}C_T^{\text{abio}}$ represents the actual fractionation-corrected ^{14}C concentration divided by $^{14}r_{\text{std}}$. This output must be saved in normalized form. But for subsequent ^{14}C budget calculations, it will be necessary to back-correct the normalized and fractionation-corrected modeled concentration ($^{14}C_T^{\text{abio}}$) and ^{14}C flux ($F_{^{14}\text{CO}_2}^{\text{abio}}$), i.e. the only two ^{14}C variables saved in OMIP, to molar units of actual ^{14}C (see Appendix A). For eventual comparison to ocean measurements, one can compute oceanic $\Delta^{14}C$ as

15   $$\Delta^{14}C_{\text{ocn}}^{\text{abio}} = 1000 \left({}^{14}r'_{\text{ocn}} - 1 \right). \tag{30}$$

For ^{13}C, the surface ocean dissolved gas concentration $\left[^{13}\text{CO}_2^*\right]$ is given by

$$\left[^{13}\text{CO}_2^*\right] = [\text{CO}_2^*]\ {}^{13}r_{\text{ocn}}, \tag{31}$$

where $^{13}r_{\text{ocn}} = {}^{13}C_T/C_T$. Here $^{13}C_T$ is not normalized by the standard ratio, but modeling groups may wish to simulate normalized $^{13}C_T$ by including a factor of $1/{}^{13}r_{\text{std}}$, analogous to what is done for the $^{14}C_T^{\text{abio}}$ normalization above.

20   2.6   Carbonate chemistry

Unlike other modelled gases in OMIP, CO_2 does not occur in seawater as a simple dissolved passive tracer. Instead, it reacts with seawater forming carbonic acid (H_2CO_3), most of which dissociates into two other inorganic species, bicarbonate (HCO_3^-) and carbonate (CO_3^{2-}) ions. Since dissolved CO_2 cannot be distinguished analytically from the much less abundant H_2CO_3, common practice is to refer to the sum of the two, $\text{CO}_2 + \text{H}_2\text{CO}_3$, as CO_2^*. The sum of the three species
25   $\text{CO}_2^* + \text{HCO}_3^- + \text{CO}_3^{2-}$ is referred to as total dissolved inorganic carbon C_T, while their partitioning depends on seawater pH, temperature, salinity, and pressure. The pH may be calculated from C_T and seawater's ionic charge balance, formalised as total alkalinity A_T. Both C_T and A_T are conservative with respect to mixing and changes in seawater temperature, salinity, and pressure. Hence both are carried as passive tracers in all ocean models, and both are used, along with temperature, salinity, and nutrient concentrations, to compute the dissolved concentration of CO_2 and the related $p\text{CO}_2$, as needed to compute air-sea
30   CO_2 fluxes.

To simulate carbonate chemistry, OMIP groups should use the total pH scale and the equilibrium constants recommended for best practices (Dickson et al., 2007; Dickson, 2010). Additionally, the model's total alkalinity equation should include alkalinity from phosphoric and silicic acid systems as well as from carbonic acid, boric acid, and water. ~~Neglect of the former two acidsystems, which we refer to as phosphorus and silicon alkalinity, is~~ namely

$$A_\mathrm{T} = A_\mathrm{C} + A_\mathrm{B} + A_\mathrm{W} + A_\mathrm{P} + A_\mathrm{SI} + A_\mathrm{O}, \tag{32}$$

where

$$A_\mathrm{C} = \left[\mathrm{HCO_3^-}\right] + 2\left[\mathrm{CO_3^{2-}}\right], \tag{33}$$

$$A_\mathrm{B} = \left[\mathrm{B(OH)_4^-}\right], \tag{34}$$

$$A_\mathrm{W} = [\mathrm{OH^-}] - [\mathrm{H^+}]_\mathrm{F} - [\mathrm{HSO_4^-}] - [\mathrm{HF}], \tag{35}$$

$$A_\mathrm{P} = \left[\mathrm{HPO_4^{2-}}\right] + 2\left[\mathrm{PO_4^{3-}}\right] - [\mathrm{H_3PO_4}], \tag{36}$$

$$A_\mathrm{SI} = \left[\mathrm{SiO(OH)_3^-}\right], \tag{37}$$

$$A_\mathrm{O} = [\mathrm{NH_3}] + [\mathrm{HS^-}] + \ldots \tag{38}$$

The right side of Eq. (32) thus separates the contributions from components of carbonic acid, boric acid, water, phosphoric acid, silicic acid, and other species, respectively. Neglect of A_P and A_SI has been common among model groups but leads to systematic errors in computed $p\mathrm{CO_2}$, e.g. in the Southern Ocean (Najjar and Orr, 1998; Orr et al., 2015). Models with the nitrogen cycle should also account for effects of changes in ~~nitrogen speciation~~ the different inorganic forms of nitrogen on total alkalinity, including changes due to denitrification and nitrogen fixation plus nitrification. ~~Models that have~~ Models with P_T ~~but not nitrogen as a nutrient should model impacts of nitrate on alkalinity by multiplying $J_{\mathrm{PO_4^{3-}}}$ by 16.~~ as the sole macronutrient tracer should consider accounting for the effect of nitrate assimilation and remineralization on alkalinity, effects that are 16 times larger than for those for P_T (Wolf-Gladrow et al., 2007).

Although phosphorus and silicon alkalinity is included in the carbonate chemistry routines provided for OCMIP2 and OCMIP3 (Orr et al., 1999b; Aumont et al., 2004), those routines focused only on computing surface $p\mathrm{CO_2}$ and are now outdated. They have been replaced by *mocsy*, a new Fortran 95 package for ocean modelers (Orr and Epitalon, 2015). Relative to the former OCMIP code, *mocsy* computes derived variables (e.g. $p\mathrm{CO_2}$, pH, $\mathrm{CO_3^{2-}}$, and $\mathrm{CaCO_3}$ saturation states) throughout the water column, corrects for common errors in pressure corrections, and replaces the solver of the pH-Alkalinity equation with the faster and safer SolveSaphe algorithm from Munhoven (2013). The latter converges under all conditions, even for very low salinity (low C_T and A_T), unlike other approaches. Although by default *mocsy* uses older scales for temperature and salinity (ITS90 and PSS78, respectively) for input, it now includes a new option so that modelers can choose to use the TEOS-10 standards (Conservative Temperature and Absolute Salinity) instead. The *mocsy* routines may be downloaded by issuing the following command:

```
git clone https://github.com/jamesorr/mocsy.git
```

and then installed by typing make. Alternatively, it can be dowloaded directly from the same site as a zipfile.

3 Diagnostics

The second goal of OMIP-BGC is to provide a complete list of diagnostics requested for the ocean simulations of in-
ert chemistry and biogeochemistry within the framework of OMIP and CMIP6. The limited diagnostics requested for the
simulations of inert chemistry are provided in Table 4. The diagnostics requested for the biogeochemical simulations are
more extensive. Hence they are given here as a series of tables separated by priority, type, and output frequency, i.e. as
annual means (Tables 5 to 8) and monthly means (Tables 9 to 16). The same list of requested variables is given in a dif-
ferent form and with more detail in the OMIP-BGC MIP tables for CMIP6, which ~~will be made available online (as an~~
~~Excel spreadsheet) from either the CMIP6 web site or the OMIP-BGC web site (see Sect. 5).~~ are available from https:
//earthsystemcog.org/projects/wip/CMIP6DataRequest.

Conceptually there is no difference in output requirements for the forced ocean simulations made for OMIP and the coupled
simulations made with the Earth System Models that are participating in CMIP6 (e.g., DECK and historical). These simulations
differ in forcing but not in the types of output requested.

To foster analysis of the model output generated by OMIP and CMIP6, OMIP-BGC plans to encourage contributions to a
centralized list of analysis subprojects. The aim is to promote collaboration while avoiding excessive redundancy to allow the
international community to advance more quickly and to exploit a greater diversity of output. Although much analysis will be
led by OMIP members, others will also be encouraged to participate, e.g., scientists from other CMIP6 projects (e.g. C4MIP)
or projects outside of CMIP (e.g., FishMIP or MAREMIP).

4 Conclusions

The required OMIP simulation *(omip1)* will be performed by many groups, each of which will couple their global-ocean, sea-
ice model to a passive-tracer transport model for inert chemistry and ocean biogeochemistry, online. All groups, even those
without biogeochemistry, will include at least one inert chemistry tracer (CFC-12) to assess subsurface model ventilation;
two other tracers (CFC-11 and SF_6) are also requested to better assess subsurface watermass ages relative to observations.
Groups with ocean biogeochemical models should also include that component (OMIP-BGC). The physical component will
be forced with the CORE II forcing (1948–2009) over five repeated cycles (310 years) as described in the companion OMIP
paper (Griffies et al., 2016). The biogeochemical component will be connected for the full 310 yr. Each model's atmospheric
CO_2 will be held to the CMIP6 preindustrial level (1 January 1850) during the first 150 years (1700–1849), while for the next
160 years (1850-2009) models will be forced to follow the historical observations as defined for CMIP6. Physical analyses will
focus on the fifth cycle, while those for the chemistry and biogeochemistry will also study transient changes over the industrial

era. ~~It is critical that all~~ All OMIP-BGC simulations ~~include~~ should include either the *natural* carbon tracer C_T^{nat}, or a parallel separate simulation that accounts only for natural carbon, in order to assess and remove effects of model drift.

An optional simulation *(omip1-spunup)* is requested from all groups having biogeochemistry and able to afford a long spin up, made beforehand. Rather than using observed climatologies to initialize the biogeochemistry as in *omip1*, this simulation

5 will be initialized with model tracer fields that have been spun up preferably for 2000 years or more. In addition, the *omip1-spunup* simulation (and its spin up) will include two simplified tracers, abiotic carbon and radiocarbon, to evaluate deep-ocean circulation and deconvolve physical vs. biological contributions to the carbon cycle. Finally, groups already having ^{13}C as a biogeochemical tracer are encouraged to include that in the *omip1-spunup* simulation (and its spin up), using commmon OMIP formulations for gas exchange and fractionation, to evaluate the simulated Suess effect and to compare cycling of ^{13}C in the

10 marine ecosystem. Besides the initial fields and the three new tracers, the *omip1* and *omip1-spunup* simulation protocols are identical.

5 Data and code availability

To facilitate comparison, an OMIP-BGC web page (http://omip-bgc.lsce.ipsl.fr), now under construction, will provide links to these protocols as well as links to distribute OMIP-BGC's common atmospheric gas histories, data fields for initialization, and

15 code to compute all facets of gas exchange and carbonate chemistry. This site will be open for public use ~~within 4 weeks after publication of this Discussion manuscript, all~~ on or before the publication of the final version of the paper. All related data files and code will be made available there~~by the time that the revised version manuscript is submitted~~. The code currently mentioned in this manuscript is available in the *mocsy* package, which can be obtained as detailed in Sect. 2.6. That package contains not only the carbonate chemistry routines, but also routines in the *gasx* module to compute Schmidt numbers, solubilities, and

20 air-sea exchange for the gases to be modeled during OMIP (CO_2, O_2, CFC-11, CFC-12, and SF_6).

Appendix A: Converting modeled ^{14}C fluxes to conventional units

The ^{14}C tracer that is adopted for OMIP from OCMIP is fractionation corrected to avoid the need to explicitly compute ^{13}C fluxes between modeled carbon reservoirs. It is also normalized. Both of these manipulations affect the units of modeled ^{14}C concentrations and fluxes. These normalized, fractionation-corrected units must be used when OMIP model groups save

25 their ^{14}C output. The saved OMIP model output is used directly to calculate simulated $\Delta^{14}C_{\text{ocn}}$ with Eqs. (29) and (30) for comparison to observations, but for budget calculations it must be converted to atoms or moles of ^{14}C (Naegler, 2009). Here we detail that conversion.

As mentioned in Sects. 2.5.3 and 2.5.4, modeled ^{14}C ratios in OMIP are expressed relative to total carbon, i.e. the *fractional isotopic abundance* $^{14}r_{\text{model}} = {}^{14}\text{C}/\text{C}$; conversely, for ^{13}C, its ratio is typically shown relative to ^{12}C (Mook, 1986), i.e. with

30 the *isotopic ratio* $^{13}R = {}^{13}\text{C}/{}^{12}\text{C}$. The *fractional abundance* approach is convenient for ocean carbon-cycle models, which already transport total carbon, e.g. to assess uptake of fossil CO_2, which includes both ^{12}C and ^{13}C. But whether ^{12}C or C

is the reference, there is only a small effect on simulated results. That is, ^{13}C amounts to only about 1% of the total carbon ($^{13}R_{std} = 0.0112372$, Craig, 1957) and ^{14}C is proportionally much less still. For ^{14}C, we adopt as a reference the standard isotopic fractional abundance $^{14}r_{std}$ (^{14}C/C) of 1.170×10^{-12}, which follows from the absolute international standard activity for $^{14}r_{std}$ of 13.56 ± 0.07 disintegrations per minute (dpm) per g C (Karlen et al., 1965) and a radiocarbon half-life of 5700 ± 30

5   yr (Audi et al., 2003; Bé et al., 2013). For comparison, Karlen et al. (1965) used the now outdated value for the half-life (5730 ± 40 yr, Godwin, 1962) to infer that $^{14}r_{std} = 1.176 \times 10^{-12}$; both of those values should now be revised downward to the values provided in the previous sentence.

The purpose of Δ^{14}C and the fractionation-normalized ratio $^{14}r_N$ is to remove the impact of isotopic fractionation to isolate the effect of ~~"aging1000~~"aging" by radioactive decay. Such fractionation occurs during photosynthesis and air-sea CO_2

10   exchange, leading to differences in the ^{13}C/^{12}C signature in different reservoirs; without fractionation, that ratio would not differ between carbon reservoirs. Fractionation of ^{14}C is about twice that of ^{13}C in permil units, based on the atomic mass difference relative to ^{12}C. One can approximately remove the influence of fractionation on ^{14}C by relying on measured δ^{13}C referenced to a common isotopic δ^{13}C signature, taken as -25‰ (Broecker and Olson, 1961). Thus for a particular reservoir i where $^{14}r_i = {}^{14}$C/C:

15   $$^{14}r_{N,i} = {}^{14}r_i \left[1 - 2 \left(\frac{\delta^{13}C_i + 25}{1000} \right) \right], \tag{A1}$$

where the two terms in the numerator in parentheses are in permil, and

$$\Delta^{14}C_i = \left(\frac{{}^{14}r_{N,i}}{{}^{14}r_{std}} - 1 \right) 1000. \tag{A2}$$

Deviations between this correction and the actual impact of fractionation on ^{14}C occur under non-steady state conditions. More importantly, radioactive decay in the ocean results in a net transfer of ^{14}C into the ocean, unlike the case for ^{13}C, and this

20   net ^{14}C flux is not corrected for fractionation. In OMIP, we simplify equations and avoid small numerical values by defining $^{14}r' = {}^{14}r/{}^{14}r_{std}$, i.e. compare Eq. (A2) with Eq. (30). This normalization is further discussed in Sects. 2.5.3 and 2.5.4 (see in particular in Eqs. (19) and (29)).

Thus OMIP simulates a ^{14}C concentration that is (1) fractionation corrected and (2) normalized by dividing ^{14}r by $^{14}r_{std}$. These corrections must be removed to convert modeled concentrations into number of atoms or moles of ^{14}C. Thus, we

25   rearrange Eq. (A1) while multiplying by the common denominator (C) of both its ^{14}r values and then we multiply by $^{14}r_{std}$, yielding

$$^{14}C = \left({}^{14}C_{model} / \left[1 - 2 \left(\frac{(\delta^{13}C + 25)}{1000} \right) \right] \right) {}^{14}r_{std}. \tag{A3}$$

Here we neglect that the δ^{13}C of the standard material (-19‰, Karlen et al., 1965) differs from that of ocean water (-1 to 2‰) because the resulting bias in computed ^{14}C is only 0.02 %.

30   Now let us use Eq. (A3) to compute corrections for the preindustrial ocean and atmosphere by plugging in their estimated δ^{13}C values. For the preindustrial ocean, we assume that δ^{13}C was around 2‰ in surface waters and 0‰ in the deep ocean, a

difference attributable to biological fractionation. Inserting those numbers into Eq. (A3) and simplifying, we thus have

$$^{14}C_S \approx {}^{14}C_{\text{model},S} \left(1 + \frac{54}{1000}\right) {}^{14}r_{\text{std}} \tag{A4a}$$

$$^{14}C_D \approx {}^{14}C_{\text{model},D} \left(1 + \frac{50}{1000}\right) {}^{14}r_{\text{std}}, \tag{A4b}$$

where the subscripts S and D indicate surface and deep waters. Thus, there is a correction of 54‰ for the surface ocean and 50‰ for the deep ocean. For the preindustrial atmosphere, using the same approach with its assumed $\delta^{13}C$ of -6.4‰, we find

$$^{14}C_A \approx {}^{14}C_{\text{model},A} \left(1 + \frac{37}{1000}\right) {}^{14}r_{\text{std}}. \tag{A5}$$

Thus, the $^{14}C_A$ correction to switch from model to conventional units for the atmosphere is about 37‰.

Turning to the gas exchange, in the model formulation the related change in the atmospheric ^{14}C inventory is calculated by removing the net air-to-sea flux $F_{^{14}CO_2}^{\text{abio}}$ and adding that to the ocean ^{14}C inventory. To convert this modeled air-sea flux into atomic units, we use the same correction as for the modeled concentrations because the change in inventory is proportional to the change in concentrations. The difference between the atmospheric and oceanic corrections ($54 - 37 = 17‰$) is related to the equilibrium fractionation factor for air-sea transfer, i.e. 8–9‰ for ^{13}C and double that for ^{14}C. In the model, the impact of fractionation on the net (non-zero) radiocarbon transfer is not taken explicitly into account giving rise to this inconsistency even under equilibrium conditions where a climatological average flux replaces the ocean sink by radioactive decay.

In the OMIP simulations, atmospheric radiocarbon is prescribed and forces the ocean. The ocean radiocarbon inventory changes in response to this forcing. Thus, a correction of about $+50‰$ (Eqs. (A4a) and (A4b)) is needed to convert ocean ^{14}C concentrations and net air-sea ^{14}C fluxes from model units into molar units. For concentrations,

$$^{14}C_{\text{T}} = {}^{14}C_{\text{T, model}}^{\text{abio}} \times 1.05 \times 1.170 \times 10^{-12}, \tag{A6}$$

and for fluxes,

$$F_{^{14}CO_2} = F_{^{14}CO_2,\text{model}}^{\text{abio}} \times 1.05 \times 1.170 \times 10^{-12}. \tag{A7}$$

In both Eqs. (A6) and (A7), units on the left-hand side are in terms of mol ^{14}C while those for the first term on the right-hand side are model units (*normalized* and *fractionation-corrected* mol ^{14}C).

References

Audi, G., Bersillon, O., Blachot, J., and Wapstra, A. H.: The NUBASE evaluation of nuclear and decay properties, Nuclear Physics A, 729, 3–128, 2003.

Aumont, O. and Bopp, L.: Globalizing results from ocean in situ iron fertilization studies,, Global Biogeochem. Cycles,, 20, GB2017, doi:10.1029/2005GB002591, 2006.

Aumont, O., Orr, J. C., Jamous, D., Monfray, P., Marti, O., and Madec, G.: A degradation approach to accelerate simulations to steady state in a 3-D tracer transport model of the global ocean, Clim. Dyn., 14, 101–116, 1998.

Aumont, O., Quéré, C. L., and Orr, J. C.: NOCES Interannual HOWTO. Internal NOCES/OCMIP report, LSCE/CEA Saclay, Gif-sur-Yvette, France, 2nd edn., http://ocmip5.ipsl.jussieu.fr/OCMIP/phase3/simulations/NOCES/HOWTO-NOCES.html, 2004.

Bacastow, R. and Maier-Reimer, E.: Ocean-circulation model of the carbon cycle, Clim. Dyn., 4, 95–125, 1990.

Bé, M., Chisté, V., Dulieu, C., Mougeot, X., Chechev, V., Kondev, F., Nichols, A., Huang, X., and Wang, B.: Table of Radionuclides (Comments on evaluations), Monographie BIPM-5, vol. 7, Bureau International des Poids et Mesure, Pavillon de Breteuil, Sèvres, France, 2013.

Bopp, L., Resplandy, L., Orr, J. C., Doney, S. C., Dunne, J. P., Gehlen, M., Halloran, P., Heinze, C., Ilyina, T., Séférian, R., Tjiputra, J., and Vichi, M.: Multiple stressors of ocean ecosystems in the 21st century: projections with CMIP5 models, Biogeosciences, 10, 6225–6245, doi:10.5194/bg–10–6225–2013, http://www.biogeosciences.net/10/6225/2013/, 2013.

Broecker, W. and Peng, T.: Tracers in the sea, Eldigio, Lamont-Doherty, Palisades, NY, 691pp, 1982.

Broecker, W., Peacock, S., Walker, S., Weiss, R., Fahrbach, E., Schröder, M., Mikolajewicz, U., Heinze, C., Key, R., Peng, T.-H., et al.: How much deep water is formed in the Southern Ocean?, Journal of Geophysical Research: Oceans, 103, 15 833–15 843, 1998.

Broecker, W. S. and Olson, E. A.: Lamont radiocarbon measurements VIII, Radiocarbon, 3, 176–204, 1961.

Broecker, W. S. and Peng, T.-H.: Gas exchange rates between air and sea, Tellus, 26, 21–35, 1974.

Bullister, J.: Atmospheric Histories (1765-2015) for CFC-11, CFC-12, CFC-113, CCl4, SF6 and N2O, Carbon Dioxide Information Analysis Center, Oak Ridge National Laboratory, U.S. Department of Energy, Oak Ridge, Tennessee, http://cdiac.ornl.gov/ftp/oceans/CFC_ATM_Hist/CFC_ATM_Hist_2015, 2015.

Bullister, J. L., Wisegarver, D. P., and Menzia, F. A.: The solubility of sulfur hexafluoride in water and seawater, Deep-Sea Res. I, 49, 175–187, 2002.

Craig, H.: Isotopic standards for carbon and oxygen and correction factors for mass-spectrometric analysis of carbon dioxide, Geochim. Cosmochim. Acta, 12, 133–149, 1957.

Dickson, A. G.: The carbon dioxide system in seawater: equilibrium chemistry and measurements, in: Guide to best practices for ocean acidification research and data reporting, edited by Riebesell, U., Fabry, V. J., Hansson, L., and Gattuso, J.-P., pp. 17–40, Publications Office of the European Union, 2010.

Dickson, A. G., Sabine, C. L., and Christian, J. R.: Guide to best practices for ocean CO_2 measurements, , PICES Special Publication 3, 191 pp., http://aquaticcommons.org/1443/, 2007.

Dlugokencky, E. and Tans, P.: Trends in atmospheric carbon dioxide, National Oceanic & Atmospheric Administration, Earth System Research Laboratory (NOAA/ESRL), available at: http://www.esrl.noaa.gov/gmd/ccgg/trends, 2016.

Doney, S., Lindsay, K., Caldeira, K., Campin, J.-M., Drange, H., Dutay, J.-C., Follows, M., Gao, Y., Gnanadesikan, A., Gruber, N., Ishida, A., Joos, F., Madec, G., Maier-Reimer, E., Marshall, J., Matear, R., Monfray, P., Mouchet, A., Najjar, R., Orr, J., Plattner, G.-K., Sarmiento,

J., Schlitzer, R., Slater, R., Totterdell, I., Weirig, M.-F., Yamanaka, Y., and Yool, A.: Evaluating Global Ocean Carbon Models: The Importance of Realistic Physics, Global Biogeochem. Cy., 18, GB3017, doi:10.1029/2003GB002150, 2004.

Dufour, C. O., Sommer, J. L., Gehlen, M., Orr, J. C., Molines, J.-M., Simeon, J., and Barnier, B.: Eddy compensation and controls of the enhanced sea-to-air CO2 flux during positive phases of the Southern Annular Mode, Global Biogeochem. Cycles, 27, 950–961, doi:10.1002/gbc.20 090, 2013.

Dutay, J.-C., Bullister, J., Doney, S. C., Orr, J. C., Najjar, R. G., Caldeira, K., Campin, J.-M., Drange, H., Follows, M., Gao, Y., Gruber, N., Hecht, M. W., Ishida, A., Joos, F., Lindsay, K., Madec, G., Maier-Reimer, E., Marshall, J. C., Matear, R., Monfray, P., Mouchet, A., Plattner, G. K., Sarmiento, J. L., Schlitzer, R., Slater, R. D., Totterdell, I. J., Weirig, M.-F., Yamanaka, Y., and Yool, A.: Evaluation of ocean model ventilation with CFC-11: Comparison of 13 global ocean models, Ocean Modelling, 4, 89–120, 2002.

Dutay, J.-C., Jean-Baptiste, P., Campin, J.-M., Ishida, A., Maier-Reimer, E., Matear, R., Mouchet, A., Totterdell, I., Yamanaka, Y., Rodgers, K., Madec, G., and Orr, J.: Evaluation of OCMIP-2 ocean models' deep circulation with mantle helium-3, J. Mar. Systems, 48, 15–36, doi:10.1016/j.jmarsys.2003.05.010, doi:10.1016/j.jmarsys.2003.05.010, 2004.

Eyring, V., Bony, S., Meehl, G. A., Senior, C. A., Stevens, B., Stouffer, R. J., and Taylor, K. E.: Overview of the Coupled Model Intercomparison Project Phase 6 (CMIP6) experimental design and organization, Geoscientific Model Development, 9, 1937–1958, doi:10.5194/gmd–9–1937–2016, 2016.

Garcia, H. E. and Gordon, L. I.: Oxygen solubility in seawater: Better fitting equations, Limnol. Oceanogr., 37, 1307–1312, 1992.

Garcia, H. E., Locarnini, R. A., Boyer, T. P., Antonov, J. I., Baranova, O., Zweng, M., Reagan, J., and Johnson, D.: World Ocean Atlas 2013, Volume 3: Dissolved Oxygen, Apparent Oxygen Utilization, and Oxygen Saturation, edited by S. Levitus and A. Mishonov, Atlas NESDIS 75, NOAA, U.S. Government Printing Office, Washington, D.C., 27 pp., 2014a.

Garcia, H. E., Locarnini, R. A., Boyer, T. P., Antonov, J. I., Baranova, O., Zweng, M., Reagan, J., and Johnson, D.: World Ocean Atlas 2013, Volume 4: Dissolved Inorganic Nutrients (phosphate, nitrate, silicate), edited by S. Levitus and A. Mishonov, Atlas NESDIS 76, NOAA, U.S. Government Printing Office, Washington, D.C., 25 pp., 2014b.

Godwin, H.: Half-life of radiocarbon, Nature, 195, 984, 1962.

Graven, H. D., Gruber, N., Key, R., Khatiwala, S., and Giraud, X.: Changing controls on oceanic radiocarbon: New insights on shallow-to-deep ocean exchange and anthropogenic CO2 uptake, J. Geophys. Res., 117, C10 005, doi:10.1029/2012JC008 074, http://dx.doi.org/10.1029/2012JC008074, 2012.

Griffies, S. M., Danabasoglu, G., Durack, P. J., Adcroft, A. J., Balaji, V., Böning, C. W., Chassignet, E. P., Curchitser, E., Deshayes, J., Drange, H., Fox-Kemper, B., Gleckler, P. J., Gregory, J. M., Haak, H., Hallberg, R. W., Heimbach, P., Hewitt, H. T., Holland, D. M., Ilyina, T., Jungclaus, J. H., Komuro, Y., Krasting, J. P., Large, W. G., Marsland, S. J., Masina, S., McDougall, T. J., Nurser, A. J. G., Orr, J. C., Pirani, A., Qiao, F., Stouffer, R. J., Taylor, K. E., Treguier, A. M., Tsujino, H., Uotila, P., Valdivieso, M., Wang, Q., Winton, M., and Yeager, S. G.: OMIP contribution to CMIP6: experimental and diagnostic protocol for the physical component of the Ocean Model Intercomparison Project, Geosci. Model Dev., 9, 3231–3296,doi:10.5194/gmd–9–3231–2016, 2016.

Hansell, D. A., Carlson, C. A., Repeta, D. J., and Schlitzer, R.: Dissolved organic matter in the ocean: A controversy stimulates new insights, Oceanography, 22, 202–211, 2009.

Jahn, A., Lindsay, K., Giraud, X., Gruber, N., Otto-Bliesner, B. L., Liu, Z., and Brady, E. C.: Carbon isotopes in the ocean model of the Community Earth System Model (CESM1), Geoscientific Model Development, 8, 2419–2434, doi:10.5194/gmd–8–2419–2015, http://www.geosci-model-dev.net/8/2419/2015/, 2015.

Jones, C. D., Arora, V., Friedlingstein, P., Bopp, L., Brovkin, V., Dunne, J., Graven, H., Hoffman, F., Ilyina, T., John, J. G., Jung, M., Kawamiya, M., Koven, C., Pongratz, J., Raddatz, T., Randerson, J., and Zaehle, S.: The C4MIP experimental protocol for CMIP6, Geosci. Model Dev., submitted, 2016.

Joos, F., Orr, J. C., and Siegenthaler, U.: Ocean carbon transport in a box-diffusion versus a general circulation model, J. Geophys. Res., 102, 12 367–12 388, 1997.

Karlen, I., Olsson, I., Kallberg, P., and Kilicci, S.: Absolute determination of the activity of two C-14 dating standards, Arkiv Geofysik., 4, 465–471, 1965.

Keeling, C. D., Piper, S. C., Bacastow, R. B., Wahlen, M., Whorf, T. P., Heimann, M., and Meijer, H. A.: Exchanges of Atmospheric CO_2 and $13CO_2$ with the Terrestrial Biosphere and Oceans from 1978 to 2000. I. Global Aspects, SIO Reference Series 01-06, Scripps Institution of Oceanography, San Diego, 2001.

Key, R. M., Sabine., C. L., Lee, K., Wanninkhof, R., Bullister, J., Feely, R. A., Millero, F. J., Mordy, C., and Peng, T.-H.: A Global Ocean Carbon Climatology: Results from Global Data Analysis Project (GLODAP), Global Biogeochem. Cy., 18, GB4031, doi:10.1029/2004GB002247, 2004.

Khatiwala, S.: Fast spin up of ocean biogeochemical models using matrix-free Newton–Krylov, Ocean Modelling, 23, 121–129, 2008.

Kwiatkowski, L., Yool, A., Allen, J. I., Anderson, T. R., Barciela, R., Buitenhuis, E. T., Butenschön, M., Enright, C., Halloran, P. R., Le Quéré, C., de Mora, L., Racault, M.-F., Sinha, B., Totterdell, I. J., and Cox, P. M.: iMarNet: an ocean biogeochemistry model intercomparison project within a common physical ocean modelling framework, Biogeosciences, 11, 7291–7304, doi:10.5194/bg–11–7291–2014, 2014.

Large, W. G. and Yeager, S. G.: The global climatology of an interannually varying air–sea flux data set, Climate Dynamics, 33, 341–364, 2009.

Lauvset, S. K., Key, R. M., Olsen, A., van Heuven, S., Velo, A., Lin, X., Schirnick, C., Kozyr, A., Tanhua, T., Hoppema, M., Jutterström, S., Steinfeldt, R., Jeansson, E., Ishii, M., Perez, F. F., Suzuki, T., and Watelet, S.: A new global interior ocean mapped climatology: the $1°$x $1°$GLODAP version 2, Earth Syst. Sci. Data Discuss., in review, 1–30, doi:10.5194/essd–2015–43, 2016.

Levin, I., Naegler, T., Kromer, B., Diehl, M., Francey, R. J., Gomez-Pelaez, A. J., Steele, L., Wagenbach, D., Weller, R., and Worthy, D. E.: Observations and modelling of the global distribution and long-term trend of atmospheric $14CO_2$, Tellus B, 62, 26–46, 2010.

Li, X. and Primeau, F. W.: A fast Newton–Krylov solver for seasonally varying global ocean biogeochemistry models, Ocean Modelling, 23, 13–20, 2008.

Lovenduski, N. S., McKinley, G. A., Fay, A. R., Lindsay, K., and Long, M. C.: Partitioning uncertainty in ocean carbon uptake projections: Internal variability, emission scenario, and model structure, Global Biogeochemical Cycles, 30, doi:10.1002/2016GB005 426, 1276–1287, 2016.

Matsumoto, K., Sarmiento, J. L., Key, R. M., Aumont, O., Bullister, J. L., Caldeira, K., Campin, J.-M., Doney, S. C., Drange, H., Dutay, J.-C., Follows, M., Gao, Y., Gnanadesikan, A., Gruber, N., Ishida, A., Joos, F., Lindsay, K., Maier-Reimer, E., Marshall, J. C., Matear, R. J., Monfray, P., Mouchet, A., Najjar, R., Plattner, G.-K., Schlitzer, R., Slater, R., Swathi, P. S., Totterdell, I. J., Weirig, M.-F., Ya-manaka, Y., Yool, A., and Orr, J. C.: Evaluation of ocean carbon cycle models with data-based metrics, Geophys. Res. Lett., 31, L070303, doi:10.1029/2003GL018970, 2004.

Meinshausen, M., Vogel, E., Nauels, A., Lorbacher, K., Etheridge, D., Trudinger, C., Rayner, P., Fraser, P., Cannadell, P., Enting, I., and et al.: Historical greenhouse gas concentrations for CMIP6, Geosci. Model Dev. Disc., in prep., 2016.

Merlis, T. M. and Khatiwala, S.: Fast dynamical spin-up of ocean general circulation models using Newton–Krylov methods, Ocean Mod-elling, 21, 97–105, 2008.

Montzka, S., Fraser, P., Butler, J., Cunnold, D., Daniel, J., Derwent, R., Lal, S., McCulloch, A., Oram, D., Reeves, C., et al.: Scientific Assessment of Ozone Depletion, vol. 47, chap. Chapter 1: Controlled substances and other source gases, World Meteorol. Organ., Geneva, Switzerland, 2003.

Mook, W.: 13C in atmospheric CO2, Netherlands J. Sea Res., 20, 211–223, 1986.

5   Mouchet, A.: The ocean bomb radiocarbon inventory revisited, Radiocarbon, 55, 1580–1594, 2013.

Munhoven, G.: The mathematics of the total alkalinity—pH equation—pathway to robust and universal solution algorithms: the SolveSAPHE package v1.0.1, Geosci. Model Dev., 6, 1367–1388, doi:10.5194/gmd–6–1367–2013, 2013.

Naegler, T.: Reconciliation of excess 14C-constrained global CO2 piston velocity estimates, Tellus B, 61, 372–384, doi:10.1111/j.1600-0889.2008.00408.x, http://dx.doi.org/10.1111/j.1600-0889.2008.00408.x, 2009.

10   Najjar, R. and Orr, J.: Design of OCMIP-2 simulations of chlorofluorocarbons, the solubility pump and common biogeochemistry, Internal OCMIP Report, LSCE/CEA Saclay, Gif-sur-Yvette, France, http://ocmip5.ipsl.fr/documentation/OCMIP/phase2/simulations/design.ps, 1998.

Najjar, R. and Orr, J. C.: Biotic-HOWTO. Internal OCMIP Report, LSCE/CEA Saclay, Gif-sur-Yvette, France, 15 pp., http://ocmip5.ipsl.jussieu.fr/OCMIP/phase2/simulations/Biotic/HOWTO-Biotic.html, 1999.

15   Najjar, R. G., Jin, X., Louanchi, F., Aumont, O., Caldeira, K., Doney, S. C., Dutay, J.-C., Follows, M., Gruber, N., Joos, F., Lindsay, K., Maier-Reimer, E., Matear, R. J., Matsumoto, K., Monfray, P., Mouchet, A., Orr, J. C., Plattner, G.-K., Sarmiento, J. L., Schlitzer, R., Slater, R. D., ad Y. Yamanaka, M.-F. W., and Yool, A.: Impact of circulation on export production, dissolved organic matter, and dissolved oxygen in the ocean: Results from Phase II of the Ocean Carbon-cycle Model Intercomparison Project (OCMIP-2), Global Biogeochemical Cycles, 21, GB3007, doi:10.1029/2006GB002 857, 2007.

20   Oliver, K. I. C., Hoogakker, B. A. A., Crowhurst, S., Henderson, G. M., Rickaby, R. E. M., Edwards, N. R., and Elderfield, H.: A synthesis of marine sediment core δ^{13}C data over the last 150 000 years, Climate of the Past, 6, 645–673, doi:10.5194/cp–6–645–2010, http://www.clim-past.net/6/645/2010/, 2010.

Olsen, A., Key, R. M., van Heuven, S., Lauvset, S. K., Velo, A., Lin, X., Schirnick, C., Kozyr, A., Tanhua, T., Hoppema, M., Jutterström, S., Steinfeldt, R., Jeansson, E., Ishii, M., Pérez, F. F., and Suzuki, T.: An internally consistent data product for the world ocean: the Global Ocean Data Analysis Project, version 2 (GLODAPv2), Earth Syst. Sci. Data Discuss., in review, 1–78, doi:10.5194/essd–2015–42, 2016.

25   Orr, J. C. and Epitalon, J.-M.: Improved routines to model the ocean carbonate system: mocsy 2.0, Geosci. Model Dev., 8, 485–499, doi:10.5194/gmd–8–485–2015, 2015.

Orr, J. C., Dutay, J.-C., Najjar, R., Bullister, J., and Brockmann, P.: CFC-HOWTO. Internal OCMIP Report, LSCE/CEA Saclay, Gif-sur-Yvette, France, 12 pp., http://ocmip5.ipsl.jussieu.fr/OCMIP/phase2/simulations/CFC/HOWTO-CFC.html, 1999a.

30   Orr, J. C., Najjar, R., Sabine, C. L., and Joos, F.: Abiotic-HOWTO. Internal OCMIP Report, LSCE/CEA Saclay, Gif-sur-Yvette, France, 25 pp., http://ocmip5.ipsl.jussieu.fr/OCMIP/phase2/simulations/Abiotic/HOWTO-Abiotic.html, 1999b.

Orr, J. C., Monfray, P., Maier-Reimer, E., Mikolajewicz, U., Palmer, J., Taylor, N. K., Toggweiler, J. R., Sarmiento, J. L., Quéré, C. L., Gruber, N., Sabine, C. L., Key, R. M., and Boutin, J.: Estimates of anthropogenic carbon uptake from four three-dimensionsal global ocean models, Global Biogeochem. Cy., 15, 43–60, 2001.

35   Orr, J. C., Fabry, V. J., Aumont, O., Bopp, L., Doney, S. C., Feely, R. A., Gnanadesikan, A., Gruber, N., Ishida, A., Joos, F., Key, R. M., Lindsay, K., Maier-Reimer, E., Matear, R., Monfray, P., Mouchet, A., Najjar, R. G., Plattner, G.-K., Rodgers, K. B., Sabine, C. L., Sarmiento, J. L., Schlitzer, R., Slater, R. D., Totterdell, I. J., Weirig, M.-F., Yamanaka, Y., and Yool, A.: Anthropogenic ocean acidification over the twenty-first century and its impact on calcifying organisms, Nature, 437, doi:10.1038/nature04 095, 681–686, 2005.

27

Orr, J. C., Gattuso, J.-P., and Epitalon, J.-M.: Comparison of ten packages that compute ocean carbonate chemistry, Biogeosciences, 12, 1483–1510, doi:10.5194/bg–12–1483–2015, 2015.

Peacock, S.: Debate over the ocean bomb radiocarbon sink: Closing the gap, Global Biogeochemical Cycles, 18, GB2022, doi:10.1029/2003GB002 211, 2004.

5   Penduff, T., Juza, M., Barnier, B., Zika, J., Dewar, W. K., Treguier, A.-M., Molines, J.-M., and Audiffren, N.: Sea level expression of intrinsic and forced ocean variabilities at interannual time scales, J. Clim., 24, 5652–5670, 2011.

Quay, P., Sonnerup, R., Westby, T., Stutsman, J., and McNichol, A.: Changes in the 13C/12C of dissolved inorganic carbon in the ocean as a tracer of anthropogenic CO_2 uptake, Global Biogeochemical Cycles, 17, 1004, doi:10.1029/2001GB001 817, 2003.

Quay, P. D., Tilbrook, B., and Wong, C.: Oceanic uptake of fossil fuel CO2: Carbon-13 evidence, Science, 256, 74–79, 1992.

10 Raynaud, S., Orr, J. C., Aumont, O., Rodgers, K. B., and Yiou, P.: Interannual-to-decadal variability of North Atlantic air-sea CO_2 fluxes, Ocean Sci., 2, 43–60, http://www.copernicus.org/EGU/os/os.html, 2006.

Redfield, A. C., Ketchum, B. H., and Richards, F.: The influence of organisms on the composition of sea water, in: The Sea, edited by Hill, M. N., vol. 2, pp. 26–77, Wiley-Interscience, New York, 1963.

Rigby, M., Prinn, R. G., O'Doherty, S., Montzka, S. A., McCulloch, A., Harth, C. M., Mühle, J., Salameh, P. K., Weiss, R. F., Young,
15 D., Simmonds, P. G., Hall, B. D., Dutton, G. S., Nance, D., Mondeel, D. J., Elkins, J. W., Krummel, P. B., Steele, L. P., and Fraser, P. J.: Re-evaluation of the lifetimes of the major CFCs and CH3CCl3 using atmospheric trends, Atmospheric Chemistry and Physics, 13, 2691–2702, doi:10.5194/acp–13–2691–2013, 2013.

Rodgers, K. B., Aumont, O., Madec, G., Menkes, C., Blanke, B., Monfray, P., Orr, J. C., and Schrag, D. P.: Radiocarbon as a thermocline proxy for the eastern equatorial Pacific, Geophys. Res. Lett., 31, L14314, doi:10.1029/2004GL019764, 2004.

20 Roullet, G. and Madec, G.: Salt conservation, free surface, and varying levels: A new formulation for ocean general circulation models, J. Geophys. Res., 105, 23 927–23 942, doi:10.1029/2000JC900 089, 2000.

Rubino, M., Etheridge, D. M., Trudinger, C. M., Allison, C. E., Battle, M. O., Langenfelds, R. L., Steele, L. P., Curran, M., Bender, M., White, J. W. C., Jenk, T. M., Blunier, T., and Francey, R. J.: A revised 1000 year atmospheric δ13C-CO2 record from Law Dome and South Pole, Antarctica, J. Geophys. Res.: Atmospheres, 118, 8482–8499, doi:10.1002/jgrd.50 668, 2013.

25 Sarmiento, J. L., Monfray, P., Maier-Reimer, E., Aumont, O., Murnane, R., and Orr, J. C.: Sea-air CO_2 fluxes and carbon transport: A comparison of three ocean general circulation models, Global Biogeochem. Cy., 14, 1267–1281, 2000.

Schmitt, J., Schneider, R., Elsig, J., Leuenberger, D., Lourantou, A., Chappellaz, J., Köhler, P., Joos, F., Stocker, T. F., Leuenberger, M., et al.: Carbon isotope constraints on the deglacial CO2 rise from ice cores, Science, 336, 711–714, 2012.

Schmittner, A., Gruber, N., Mix, A. C., Key, R. M., Tagliabue, A., and Westberry, T. K.: Biology and air-sea gas exchange controls on the
30 distribution of carbon isotope ratios ($\delta^{13}C$) in the ocean, Biogeosciences, 10, 5793–2013, doi:10.5194/bg–10–5793–2013, 2013.

Séférian, R., Gehlen, M., Bopp, L., Resplandy, L., Orr, J. C., Marti, O., Dunne, J. P., Christian, J. R., Doney, S. C., Ilyina, T., Lindsay, K., Halloran, P., Heinze, C., Segschneider, J., and Tjiputra, J.: Inconsistent strategies to spin up models in CMIP5: implications for ocean biogeochemical model performance assessment, Geoscientific Model Development Discussions, 8, 8751–8808, doi:10.5194/gmdd–8–8751–2015, 2015.

35 Sweeney, C., Gloor, E., Jacobson, A. R., Key, R. M., McKinley, G., Sarmiento, J. L., and Wanninkhof, R.: Constraining global air-sea gas exchange for CO2 with recent bomb 14C measurements, Global Biogeochemical Cycles, 21, GB2015, doi:10.1029/2006GB002 784, 2007.

Tagliabue, A. and Bopp, L.: Towards understanding global variability in ocean carbon-13, Global Biogeochem. Cy., 22, GB1025, doi:10.1029/2007GB003 037, 2008.

Tagliabue, A., Aumont, O., DeAth, R., Dunne, J. P., Dutkiewicz, S., Galbraith, E., Misumi, K., Moore, J. K., Ridgwell, A., Sherman, E., et al.: How well do global ocean biogeochemistry models simulate dissolved iron distributions?, Global Biogeochem. Cy., 30, 149–174, 2015GB005 289, 10.1002/2015GB005 289, 2016.

Toggweiler, J. R., Dixon, K., and Bryan, K.: Simulations of radiocarbon in a coarse resolution world ocean model 1. Steady state prebomb distributions, J. Geophys. Res., 94, 8217–8242, 1989a.

Toggweiler, J. R., Dixon, K., and Bryan, K.: Simulations of radiocarbon in a coarse resolution world ocean model 2. Distributions of bomb-produced carbon 14, J. Geophys. Res., 94, 8243–8264, 1989b.

Walker, S. J., Weiss, R. F., and Salameh, P. K.: Reconstructed histories of the annual mean atmospheric mole fractions for the halocarbons CFC-11 CFC-12, CFC-113, and carbon tetrachloride, J. Geophys. Res., 105, 14 285–14 296, doi:10.1029/1999JC900 273, 2000.

Wanninkhof, R.: Relationship between wind speed and gas exchange over the ocean, J. Geophys. Res., 97, 7373–7382, 1992.

Wanninkhof, R.: Relationship between wind speed and gas exchange over the ocean revisited, Limnol. Oceanogr. Methods, 12, 351–362, 2014.

Warner, M. J. and Weiss, R. F.: Solubilities of chlorofluorocarbons 11 and 12 in water and seawater, Deep-Sea Res. Part A., 32, 1485–1497, 1985.

Waugh, D. W., Hall, T. M., and Haine, T. W. N.: Relationship among tracer ages, J. Geophys. Res., 108, doi:10.1029/2002JC001 325, 2003.

Weiss, R. F.: Carbon dioxide in water and seawater: the solubility of a non-ideal gas, Mar. Chem., 2, 203–215, 1974.

Weiss, R. F. and Price, B. A.: Nitrous oxide solubility in water and seawater, Mar. Chem., 8, 347–359, 1980.

Wolf-Gladrow, D. A., Zeebe, R. E., Klaas, C., Körtzinger, A., and Dickson, A. G.: Total alkalinity: The explicit conservative expression and its application to biogeochemical processes, Mar. Chem., 106, 287–300, 2007.

Yool, A., Oschlies, A., Nurser, A. J. G., and Gruber, N.: A model-based assessment of the TrOCA approach for estimating anthropogenic carbon in the ocean, Biogeosciences, 7, 723–751, doi:10.5194/bg–7–723–2010, 2010.

Zhang, J., Quay, P. D., and Wilbur, D. O.: Carbon isotope fractionation during gas-water exchange and dissolution of CO 2, Geochimica et Cosmochimica Acta, 59, 107–114, 1995.

Table 1. Seawater coefficients for fit of Sc to temperature[*,†] from Wanninkhof (2014).

Gas	A	B	C	D	E	Sc (20°C)
CFC-11	3579.2	−222.63	7.5749	−0.14595	0.0011874	1179
CFC-12	3828.1	−249.86	8.7603	−0.1716	0.001408	1188
SF_6	3177.5	−200.57	6.8865	−0.13335	0.0010877	1028
CO_2	2116.8	−136.25	4.7353	−0.092307	0.0007555	668
O_2	1920.4	−135.6	5.2122	−0.10939	0.00093777	568
N_2O	2356.2	−166.38	6.3952	−0.13422	0.0011506	697
DMS	2855.7	−177.63	6.0438	−0.11645	0.00094743	941

[*] Coefficients for fit to $Sc = A + B\,T_c + C\,T_c^2 + D\,T_c^3 + E\,T_c^4$, where T_c is surface temperature in °C

[†] Conservative Temperature should be converted to in situ temperature before using these coefficients

Table 2. Coefficients for fit[*,†,‡] of solubility function ϕ_A^0 ($\text{mol L}^{-1}\,\text{atm}^{-1}$).

Gas	a_1	a_2	a_3	a_4	b_1	b_2	b_3
CFC-11	-229.9261	319.6552	119.4471	-1.39165	-0.142382	0.091459	-0.0157274
CFC-12	-218.0971	298.9702	113.8049	-1.39165	-0.143566	0.091015	-0.0153924
SF_6	-80.0343	117.232	29.5817	0.0	0.0335183	-0.0373942	0.00774862
CO_2	-160.7333	215.4152	89.8920	-1.47759	0.029941	-0.027455	0.0053407
N_2O	-165.8806	222.8743	92.0792	-1.48425	-0.056235	0.031619	-0.0048472

[*] Fit to Eq. (15), where T is in-situ, absolute temperature (K) and S is salinity (practical salinity scale).

[†] For units of $\text{mol m}^{-3}\,\text{atm}^{-1}$, coefficients should be multiplied by 1000.

[‡] The units refer to atm of each gas, not atm of air.

[§] When using these coefficients, conservative temperature should be converted to in situ temperature (K) and absolute salinity should be converted to practical salinity.

Table 3. Coefficients for fit of K' and K_0 (both in $\mathrm{mol\,L^{-1}\,atm^{-1}}$).

Gas	a_1	a_2	a_3	b_1	b_2	b_3
				K'		
CFC-11	-134.1536	203.2156	56.2320	-0.144449	0.092952	-0.0159977
CFC-12	-122.3246	182.5306	50.5898	-0.145633	0.092509	-0.0156627
SF_6	-96.5975	139.883	37.8193	0.0310693	-0.0356385	0.00743254
				K_0		
CO_2	-58.0931	90.5069	22.2940	0.027766	-0.025888	0.0050578
N_2O	-62.7062	97.3066	24.1406	-0.058420	0.033193	-0.0051313

[*] Fit to Eq. 24, where T is in-situ, absolute temperature (K) and S is salinity (practical scale).

[†] The final three footnotes of Table 2 also apply here.

Table 4. Output for inert chemistry.

Symbol

~~CFC-11~~ SF$_6$

~~CFC-12~~ CFC-11

CFC-12

~~$F_{\text{CFC-11}}$ fgcfc11 mol m^{-2} s^{-1} XY 2 Surface Downward CFC-11 flux $F_{\text{CFC-12}}$ fgcfc12 mol m^{-2} s^{-1} XY 1 Surface Downward CFC-12 flux F_{SF_6} fgsf6~~

~~Fe*~~ CFC-11

~~Si_T~~ CFC-12

~~$F_{\text{CO}_2^{\text{tot}}}$ fgco2 kg m^{-2} s^{-1} XY 1 Surface Downward Flux of Total CO2 $F_{\text{CO}_2^{\text{nat}}}$ fgco2nat kg m^{-2} s^{-1} XY 1 Surface Downward Flux of Natural CO2 F_{CO}~~

~~$F_{14\text{CO}_2^{\text{abio}}}$~~ $F_{\text{CFC-11}}$

~~$F_{14\text{CO}_2}$~~ $F_{\text{CFC-12}}$

Table 5. Annual-mean biogeochemical output: Priority 1.

Symbol	Variable name	Units	Shape	Priority	Long name
C_T	dissic	$\mathrm{mol\ m^{-3}}$	XYZ	1	Dissolved Inorganic Carbon Concentration
$C_\mathrm{T}^{\mathrm{nat}}$	dissicnat	$\mathrm{mol\ m^{-3}}$	XYZ	1	Natural Dissolved Inorganic Carbon Concentration
$C_\mathrm{T}^{\mathrm{abio}}$	dissicabio	$\mathrm{mol\ m^{-3}}$	XYZ	1	Abiotic Dissolved Inorganic Carbon Concentration
$^{14}C_\mathrm{T}^{\mathrm{abio}}$	dissi14cabio	$\mathrm{mol\ m^{-3}}$	XYZ	1	Abiotic Dissolved Inorganic 14Carbon Concentration
$^{13}C_\mathrm{T}$	dissi13c	$\mathrm{mol\ m^{-3}}$	XYZ	1	Dissolved Inorganic 13Carbon Concentration
A_T	talk	$\mathrm{mol\ m^{-3}}$	XYZ	1	Total Alkalinity
$A_\mathrm{T}^{\mathrm{nat}}$	talknat	$\mathrm{mol\ m^{-3}}$	XYZ	1	Natural Total Alkalinity
pH	ph	1	XYZ	1	pH
$\mathrm{pH}^{\mathrm{nat}}$	phnat	1	XYZ	1	Natural pH
$\mathrm{pH}^{\mathrm{abio}}$	phabio	1	XYZ	1	Abiotic pH
O_2	o2	$\mathrm{mol\ m^{-3}}$	XYZ	1	Dissolved Oxygen Concentration
P_T	po4^{a,*}	$\mathrm{mol\ m^{-3}}$	XYZ	1	Total Dissolved Inorganic Phosphorus Concentration
Chl	chl§	$\mathrm{kg\ m^{-3}}$	XYZ	1	Mass Concentration of Total Chlorophyll in Seawater
$F_{\mathrm{CO}_2^{\mathrm{tot}}}$	fgco2	$\mathrm{kg\ m^{-2}\ s^{-1}}$	XY	1	Surface Downward Flux of Total CO2
$F_{\mathrm{CO}_2^{\mathrm{nat}}}$	fgco2nat	$\mathrm{kg\ m^{-2}\ s^{-1}}$	XY	1	Surface Downward Flux of Natural CO2
$F_{\mathrm{CO}_2^{\mathrm{abio}}}$	fgco2abio	$\mathrm{kg\ m^{-2}\ s^{-1}}$	XY	1	Surface Downward Flux of Abiotic CO2
$F_{^{14}\mathrm{CO}_2^{\mathrm{abio}}}$	fg14co2abio	$\mathrm{kg\ m^{-2}\ s^{-1}}$	XY	1	Surface Downward Flux of Abiotic 14CO2
$F_{^{14}\mathrm{CO}_2}$	fg13co2	$\mathrm{kg\ m^{-2}\ s^{-1}}$	XY	1	Surface Downward Flux of 13CO2

[a] For models that do not carry P_T as a tracer, compute it from $\mathrm{NO_3^-}$ assuming N:P = 16:1

[*] $P_\mathrm{T} = \mathrm{H_3PO_4} + \mathrm{H_2PO_4^-} + \mathrm{HPO_4^{2-}} + \mathrm{PO_4^{3-}}$. In seawater most of P_T is in the form of $\mathrm{HPO_4^{2-}}$, while $\mathrm{PO_4^{3-}}$ makes up only $\sim$10% at pH 8.

[†] dissolved iron in sea water includes both $\mathrm{Fe^{2+}}$ and $\mathrm{Fe^{3+}}$ ions (but not, e.g. particulate detrital iron)

[‡] $Si_\mathrm{T} = \left[\mathrm{Si(OH)_4}\right] + \left[\mathrm{SiO(OH)_3^-}\right]$, i.e. the sum of silicic acid and silicate

[§] sum of chlorophyll from all phytoplankton group concentrations. In most models this is equal to chldiat+chlmisc.

Table 6. Annual-mean biogeochemical output: Priority 2 (concentrations).

Symbol	Variable name	Units	Shape	Priority	Long name
NO_3^-	no3	$mol\,m^{-3}$	XYZ	2	Dissolved Nitrate Conentration
Fe^*	dfe[†]	$mol\,m^{-3}$	XYZ	2	Mole Concentration of Dissolved Iron in sea water
Si_T	si[‡]	$mol\,m^{-3}$	XYZ	2	Total Dissolved Inorganic Silicon Concentration
DOC	dissoc	$mol\,m^{-3}$	XYZ	2	Dissolved Organic Carbon Concentration
	phyc	$mol\,m^{-3}$	XYZ	2	Phytoplankton Carbon Concentration
	zooc	$mol\,m^{-3}$	XYZ	2	Zooplankton Carbon Concentration
	detoc	$mol\,m^{-3}$	XYZ	2	Detrital Organic Carbon Concentration
$[CaCO_3]_{calc}$	calc	$mol\,m^{-3}$	XYZ	2	Calcite Concentration
$[CaCO_3]_{arag}$	arag	$mol\,m^{-3}$	XYZ	2	Aragonite Concentration
$[O_2]_{sat}$	o2sat	$mol\,m^{-3}$	XYZ	2	Dissolved Oxygen Concentration at Saturation
$[NH_4^+]$	nh4	$mol\,m^{-3}$	XYZ	2	Dissolved Ammonium Concentration
	chldiat[*]	$kg\,m^{-3}$	XYZ	2	Mass Concentration of Diatom expressed as Chlorophyll in sea water
	chldiaz[†]	$kg\,m^{-3}$	XYZ	2	Mass Concentration of Diazotrophs expressed as Chlorophyll in Seawater
	chlcalc[‡]	$kg\,m^{-3}$	XYZ	2	Mass Concentration of Calcareous Phytoplankton expressed as Chlorophyll in Seawater
	chlpico[§]	$kg\,m^{-3}$	XYZ	2	Mass Concentration of Picophytoplankton expressed as Chlorophyll in sea water
	chlmisc[¶]	$kg\,m^{-3}$	XYZ	2	Mass Concentration of Other Phytoplankton expressed as Chlorophyll in sea water
	pon	$mol\,m^{-3}$	XYZ	2	Mole Concentration of Particulate Organic Matter expressed as Nitrogen in sea water
	pop	$mol\,m^{-3}$	XYZ	2	Mole Concentration of Particulate Organic Matter expressed as Phosphorus in sea water
	bfe[1]	$mol\,m^{-3}$	XYZ	2	Mole Concentration of Particulate Organic Matter expressed as Iron in sea water
	bsi[2]	$mol\,m^{-3}$	XYZ	2	Mole Concentration of Particulate Organic Matter expressed as silicon in sea water
	phyn	$mol\,m^{-3}$	XYZ	2	Mole Concentration of Total Phytoplankton expressed as Nitrogen in sea water
	phyp	$mol\,m^{-3}$	XYZ	2	Mole Concentration of Total Phytoplankton expressed as Phosphorus in sea water
	phyfe	$mol\,m^{-3}$	XYZ	2	Mole Concentration of Total Phytoplankton expressed as Iron in sea water
	physi	$mol\,m^{-3}$	XYZ	2	Mole Concentration of Total Phytoplankton expressed as Silicon in sea water
DMS	dms	$mol\,m^{-3}$	XYZ	2	Mole Concentration of Dimethyl Sulphide in sea water
$[CO_3^{2-}]$	co3	$mol\,m^{-3}$	XYZ	2	Carbonate ion Concentration
$[CO_3^{2-}]^{nat}$	co3nat	$mol\,m^{-3}$	XYZ	2	Natural Carbonate ion Concentration
$[CO_3^{2-}]^{abio}$	co3abio	$mol\,m^{-3}$	XYZ	2	Abiotic Carbonate ion Concentration
$[CO_3^{2-}]_{sat}^{calc}$	co3satcalc	$mol\,m^{-3}$	XYZ	2	Carbonate ion Concentration for sea water in equilibrium with pure Calcite
$[CO_3^{2-}]_{sat}^{arag}$	co3satarag	$mol\,m^{-3}$	XYZ	2	Carbonate ion Concentration for sea water in equilibrium with pure Aragonite

[*] chlorophyll from diatom phytoplankton component concentration alone

[†] chlorophyll concentration from the diazotrophic phytoplankton component alone

[‡] chlorophyll concentration from the calcite-producing phytoplankton component alone

[§] chlorophyll concentration from the picophytoplankton ($<2\,\mu m$) component alone

[¶] chlorophyll from additional phytoplankton component concentrations alone

Table 7. Annual-mean biogeochemical output: Priority 2 (rates).

Variable name	Units	Shape	Priority	Long name
pp	mol m^{-3} s^{-1}	XYZ	2	Primary Carbon Production by Total Phytoplankton
pnitrate	mol m^{-3} s^{-1}	XYZ	2	Primary Carbon Production by Phytoplankton due to Nitrate Uptake Alone
pbfe	mol m^{-3} s^{-1}	XYZ	2	Biogenic Iron Production
pbsi	mol m^{-3} s^{-1}	XYZ	2	Biogenic Silica Production
pcalc	mol m^{-3} s^{-1}	XYZ	2	Calcite Production
parag	mol m^{-3} s^{-1}	XYZ	2	Aragonite Production
expc	mol m^{-2} s^{-1}	XYZ	2	Sinking Particulate Organic Carbon Flux
expn	mol m^{-2} s^{-1}	XYZ	2	Sinking Particulate Organic Nitrogen Flux
expp	mol m^{-2} s^{-1}	XYZ	2	Sinking Particulate Organic Phosphorus Flux
expfe	mol m^{-2} s^{-1}	XYZ	2	Sinking Particulate Iron Flux
expsi	mol m^{-2} s^{-1}	XYZ	2	Sinking Particulate Silica Flux
expcalc	mol m^{-2} s^{-1}	XYZ	2	Sinking Calcite Flux
exparag	mol m^{-2} s^{-1}	XYZ	2	Sinking Aragonite Flux
remoc	mol m^{-3} s^{-1}	XYZ	2	Remineralization of Organic Carbon
dcalc	mol m^{-3} s^{-1}	XYZ	2	Calcite Dissolution
darag	mol m^{-3} s^{-1}	XYZ	2	Aragonite Dissolution
ppdiat	mol m^{-3} s^{-1}	XYZ	2	Diatom Primary Carbon Production

Table 8. Annual-mean biogeochemical output: Priority 3.

Variable name	Units	Shape	Priority	Long name
bacc	mol m^{-3}	XYZ	3	Bacterial Carbon Concentration
phydiat	mol m^{-3}	XYZ	3	Mole Concentration of Diatoms expressed as Carbon in ~~Seawater~~sea water
phydiaz	mol m^{-3}	XYZ	3	Mole Concentration of Diazotrophs Expressed as Carbon in ~~Seawater~~sea water
phycalc	mol m^{-3}	XYZ	3	Mole Concentration of Calcareous Phytoplankton expressed as Carbon in ~~Seawater~~sea water
phypico*	mol m^{-3}	XYZ	3	Mole Concentration of Picophytoplankton expressed as Carbon in ~~Seawater~~sea water
phymisc†	mol m^{-3}	XYZ	3	Mole Concentration of Miscellaneous Phytoplankton expressed as Carbon in ~~Seawater~~sea water
zmicro‡	mol m^{-3}	XYZ	3	Mole Concentration of Microzooplankton expressed as Carbon in ~~Seawater~~sea water
zmeso§	mol m^{-3}	XYZ	3	Mole Concentration of Mesozooplankton expressed as Carbon in ~~Seawater~~sea water
zmisc¶	mol m^{-3}	XYZ	3	Mole ~~Concetration~~ Concentration of Other Zooplankton ~~Carbon Concentration~~ expressed as Carbon in ~~Seawater~~sea water
~~ppdiaz~~ dpocdtdiaz	mol m^{-3} s^{-1}	XYZ	3	Tendency of Mole Concentration of Organic Carbon in ~~Seawater~~sea water due to NPP by Diazotrophs
~~ppcalc~~ dpocdtcalc	mol m^{-3} s^{-1}	XYZ	3	Tendency of Mole Concentration of Organic Carbon in ~~Seawater~~sea water due to NPP by Calcareous Phytoplankton
~~pppico~~ dpocdtpico	mol m^{-3} s^{-1}	XYZ	3	Tendency of Mole Concentration of Organic Carbon in ~~Seawater~~sea water due to NPP by Picophytoplankton
~~ppmisc~~ ppdiat	mol m^{-3} s^{-1}	XYZ	3	~~Other Phytoplankton Carbon Production~~ Net Primary Organic Carbon Production by Diatoms
ppdiaz	mol m^{-3} s^{-1}	XYZ	3	Net Primary Mole Productivity of Carbon by Diazotrophs
ppcalc	mol m^{-3} s^{-1}	XYZ	3	Net Primary Mole Productivity of Carbon by Calcareous Phytoplankton
pppico	mol m^{-3} s^{-1}	XYZ	3	Net Primary Mole Productivity of Carbon by Picophytoplankton
ppmisc	mol m^{-3} s^{-1}	XYZ	3	Net Primary Organic Carbon Production by Other Phytoplankton
bddtdic	mol m^{-3} s^{-1}	XYZ	3	Rate of Change of Dissolved Inorganic Carbon due to Biological Activity
bddtdin	mol m^{-3} s^{-1}	XYZ	3	Rate of Change of Nitrogen Nutrient due to Biological Activity
bddtdip	mol m^{-3} s^{-1}	XYZ	3	Rate of Change of ~~Total~~ Dissolved Phosphorus due to Biological Activity
bddtdife	mol m^{-3} s^{-1}	XYZ	3	Rate of Change of Dissolved Inorganic Iron due to Biological Activity
bddtdisi	mol m^{-3} s^{-1}	XYZ	3	Rate of Change of Total Dissolved Inorganic Silicon due to Biological Activity
bddtalk	mol m^{-3} s^{-1}	XYZ	3	Rate of Change of Alkalinity due to Biological Activity
fescav	mol m^{-3} s^{-1}	XYZ	3	Nonbiogenic Iron Scavenging
fediss	mol m^{-3} s^{-1}	XYZ	3	Particle Source of Dissolved Iron
graz	mol m^{-3} s^{-1}	XYZ	3	Total Grazing of Phytoplankton by Zooplankton

* carbon concentration from the picophytoplankton (<2 μm) component alone

† carbon concentration from additional phytoplankton component alone

‡ carbon concentration from the microzooplankton (<20 μm) component alone

§ carbon concentration from mesozooplankton (20–200 μm) component alone

¶ carbon from additional zooplankton component concentrations alone (e.g, micro, meso). Provides check for model intercomparison since some phytoplankton groups are supersets.

Table 9. Monthly mean biogeochemical output: Priority 1.

Symbol	Variable name	Units	Shape	Priority	Long name
	dissicos	mol m^{-3}	XY	1	Surface Dissolved Inorganic Carbon Concentration
	dissicnatos	mol m^{-3}	XY	1	Surface Natural Dissolved Inorganic Carbon Concentration
	dissicabioos	mol m^{-3}	XY	1	Surface Abiotic Dissolved Inorganic Carbon Concentration
	dissi14cabioos	mol m^{-3}	XY	1	Surface Abiotic Dissolved Inorganic 14Carbon Concentration
	dissi13cos	mol m^{-3}	XY	1	Surface Dissolved Inorganic 13Carbon Concentration
	talkos	mol m^{-3}	XY	1	Surface Total Alkalinity
	talknatos	mol m^{-3}	XY	1	Surface Natural Total Alkalinity
	phos	1	XY	1	Surface pH
	o2os	mol m^{-3}	XY	1	Surface Dissolved Oxygen Concentration
	o2satos	mol m^{-3}	XY	1	Surface Dissolved Oxygen Concentration at Saturation
	po4os	mol m^{-3}	XY	1	Surface Total Dissolved Inorganic Phosphorus Concentration
	chlos	kg m^{-3}	XY	1	Surface Mass Conc. of Total Phytoplankton expressed as Chlorophyll in sea water
C_{T}	dissic	mol m^{-3}	XYZ	1	Dissolved Inorganic Carbon Concentration
A_{T}	talk	mol m^{-3}	XYZ	1	Total Alkalinity
P_{T}	po4^a	mol m^{-3}	XYZ	1	Total Dissolved Inorganic Phosphorus Concentration
	intpp*	mol m^{-2} s^{-1}	XY	1	Primary Organic Carbon Production by All Types of Phytoplankton
	expc100†	mol m^{-2} s^{-1}	XY	1	Downward Flux of Particle Organic Carbon
	expcalc100†	mol m^{-2} s^{-1}	XY	1	Downward Flux of Calcite
	exparag100†	mol m^{-2} s^{-1}	XY	1	Downward Flux of Aragonite
$p\mathrm{CO}_2$	spco2	Pa	XY	1	Surface Aqueous Partial Pressure of CO2
$p\mathrm{CO}_2^{\mathrm{nat}}$	spco2nat	Pa	XY	1	Natural Surface Aqueous Partial Pressure of CO2
$p\mathrm{CO}_2^{\mathrm{abio}}$	spco2abio	Pa	XY	1	Abiotic Surface Aqueous Partial Pressure of CO2
$F_{\mathrm{CO}_2^{\mathrm{tot}}}$	fgco2	kg m^{-2} s^{-1}	XY	1	Surface Downward Flux of Total CO2
$F_{\mathrm{CO}_2^{\mathrm{nat}}}$	fgco2nat	kg m^{-2} s^{-1}	XY	1	Surface Downward Flux of Natural CO2
$F_{\mathrm{CO}_2^{\mathrm{abio}}}$	fgco2abio	kg m^{-2} s^{-1}	XY	1	Surface Downward Flux of Abiotic CO2
$F_{^{14}\mathrm{CO}_2^{\mathrm{abio}}}$	fg14co2abio	kg m^{-2} s^{-1}	XY	1	Surface Downward Flux of Abiotic 14CO2
$F_{^{14}\mathrm{CO}_2}$	fg13co2	kg m^{-2} s^{-1}	XY	1	Surface Downward Flux of 13CO2
F_{O_2}	fgo2	mol m^{-2} s^{-1}	XY	1	Surface Downward Flux of O2

^{a} For models that do not carry P_{T} as a tracer, compute it from NO_3^- assuming N:P $= 16$:1

* Vertically integrated total primary (organic carbon) production by phytoplankton. This should equal the sum of intpdiat+intpphymisc, but those individual components may be unavailable in some models.

† at 100-m depth

‡ modeled dissolved iron includes all simulated dissolved species, both free and organically complexed

Table 10. Monthly mean biogeochemical output: Priority 2 (2-D fields).

Symbol	Variable name	Units	Shape	Priority	Long name
C_T	~~dissic~~ dissocos	mol m^{-3}	~~XYZ~~ XY	~~1~~ 2	~~Dissolved Inorganic~~ Surface Dissolved Organic Carbon Concentration
C_T^{nat}	~~dissicnat~~ phycos	mol m^{-3}	~~XYZ~~ XY	~~1~~ 2	~~Natural Dissolved Inorganic~~ Surface Phytoplankton Carbon Concentration
C_T^{abio}	~~dissicabio~~ zoocos	mol m^{-3}	~~XYZ~~ XY	~~1~~ 2	~~Abiotic Dissolved Inorganic~~ Surface Zooplankton Carbon Concentration
$^{14}C_T^{abio}$	~~dissi14cabio~~ detocos	mol m^{-3}	~~XYZ~~ XY	~~1~~ 2	~~Abiotic Dissolved Inorganic 14Carbon~~ Surface Detrital Organic Carbon
$^{13}C_T$	~~dissi13c~~ calcos	mol m^{-3}	~~XYZ~~ XY	~~1~~ 2	~~Dissolved Inorganic 13Carbon~~ Surface Calcite Concentration
A_T	~~talk~~ aragos	mol m^{-3}	~~XYZ~~ XY	2	Surface Aragonite Concentration
	phos	1	~~Total Alkalinity~~ XY	2	Surface pH
A_T^{nat}	~~talknat~~ phnatos	~~1~~	XY	2	Surface Natural pH
	phabioos	~~1~~	XY	2	Surface Abiotic pH
O_2	no3os	mol m^{-3}	~~XYZ~~ XY	~~1~~ 2	~~Natural Total Alkalinity~~ Surface Dissolved Nitrate Concentration
NO_3^-	~~o2~~ nh4os	mol m^{-3}	~~XYZ~~ XY	~~1~~ 2	~~Dissolved Oxygen~~ Surface Dissolved Ammonium Concentration
P_T	~~no3~~ dfeos	mol m^{-3}	~~XYZ~~ XY	~~1~~ 2	~~Dissolved Nitrate~~ Surface Dissolved Iron Concentration
Fe	~~po4~~ sios	mol m^{-3}	~~XYZ~~ XY	~~1~~ 2	Surface Total Dissolved Inorganic ~~Phosphorus~~ Silicon Concentration
Si_T	~~dfe~~ co3os	mol m^{-3}	~~XYZ~~ XY	~~1~~ 2	~~Dissolved Iron~~ Surface Carbonate ion Concentration
Chl	~~si~~ co3natos	mol m^{-3}	~~XYZ~~ XY	~~1~~ 2	~~Total Dissolved Inorganic Silicon~~ Surface Natural Carbonate ion Concentration
pH	~~eh~~ co3abioos	~~kg~~ mol m^{-3}	~~XYZ~~ XY	~~1~~ 2	~~Total Chlorophyll Mass~~ Surface Abiotic Carbonate ion Concentration
pH^{nat}	~~ph~~ co3satcalcos	~~1~~ mol m^{-3}	~~XYZ~~ XY	~~1~~ 2	~~pH~~ Surface Mole Concentration of Dimethyl Sulphide in sea water
pH^{abio}	~~phnat~~ co3sataragos	~~1~~ mol m^{-3}	~~XYZ~~ XY	2	Surface Mole Concentration of Dimethyl Sulphide in sea water
	limndiat[1]	1	~~Natural pH~~ XY	2	Nitrogen limitation of Diatoms
	~~phabio~~ limirrdiat[1]	1	~~XYZ~~ XY	2	Irradiance limitation of Diatoms
	limfediat[1]	1	~~Abiotic pH~~ XY	2	Iron limitation of Diatoms
	~~intpp~~ intppnitrate*	mol m^{-2} s^{-1}	XY	~~1~~ 2	Primary Organic Carbon Production by ~~All Types of Phytoplankton~~ Phy...
	~~expc100~~ intppdiat†	mol m^{-2} s^{-1}	XY	~~1~~ 2	~~Downward Flux of Particle Organic Carbon~~ Primary Organic Carbon Pro...
$\int C_T\,dz$	~~expcalc100~~ intdic‡	~~mol~~ kg m^{-2} ~~s^{-1}~~	XY	~~1~~ 2	~~Downward Flux of Calcite~~ Dissolved Inorganic Carbon Content
$\int DOC\,dz$	~~exparag100~~ intdoc§	~~mol~~ kg m^{-2} ~~s^{-1}~~	XY	~~1~~ 2	~~Downward Flux of Aragonite~~ Dissolved Organic Carbon Content
$\rho\int POC\,dz$	~~spco2~~ intpoc¶	Pa kg m^{-2}	XY	~~1~~ 2	~~Surface Aqueous Partial Pressure of CO2~~ Particulate Organic Carbon Co...
~~p~~ height					

[1] These 2-D limitation terms should be calculated as the carbon biomass weighted average for the upper 100 m
* Vertically integrated primary (organic carbon) production by phytoplankton based on nitrate uptake alone
† Vertically integrated primary (organic carbon) production by the diatom phytoplankton component alone
‡ Vertically integrated C_T
§ Vertically integrated DOC (explicit pools only)
¶ Vertically integrated POC

Table 11. Monthly mean biogeochemical output: Priority 2 (3-D fields).

Symbol	Variable name	Units	Shape
C_T^{nat}	dissicnat	mol m^{-3}	XYZ
pC_T^{abio}	~~spco2abio~~ dissicabio	~~Pa~~ mol m^{-3}	~~XY~~-XYZ
$F_{\text{CO}_2}^{\text{nat}-14}C_T^{\text{abio}}$	~~fgco2~~ dissi14cabio	~~kg m^{-2} s^{-1}~~ mol m^{-3}	~~XY~~-XYZ
$F_{\text{CO}_2}^{\text{nat}-13}C_T$	~~fgco2nat~~ dissi13c	~~kg m^{-2} s^{-1}~~ mol m^{-3}	~~XY~~-XYZ
$F_{\text{CO}_2}^{\text{abio}-}A_T^{\text{nat}}$	~~fgco2abio~~ talknat	~~kg m^{-2} s^{-1}~~ mol m^{-3}	~~XY~~-XYZ
pH	ph	1	Surface Downward Flux of Abiotic
$F_{14\text{CO}_2}^{\text{abio}-}pH^{\text{nat}}$	~~fg14co2abio~~ phnat	~~kg m^{-2} s^{-1}~~ 1	~~XY~~-XYZ
pH$^{\text{abio}}$	phabio	1	Surface Downward Flux of Abiotic
$F_{14\text{CO}_2-}\text{O}_2$	~~fg13co2~~ o2	~~kg m^{-2} s^{-1}~~ mol m^{-3}	~~XY~~-XYZ
F_{O_2}	~~fgo2~~ o2sat	mol m^{-2} s^{-1} $^{-3}$	~~XY~~-XYZ
~~Monthly mean biogeochemical output: Priority 2. Symbol~~-NO$_3^-$	~~Variable name~~ no3	~~Units~~ mol m^{-3}	~~Shape~~-XYZ
$[\text{NH}_4^+]$	nh4	mol m^{-3}	XYZ
Fe‡	dfe	mol m^{-3}	XYZ
Si_T	si	mol m^{-3}	XYZ
Chl	chl	kg m^{-3}	XYZ
DOC	dissoc	mol m^{-3}	XYZ
	phyc	mol m^{-3}	XYZ
	zooc	mol m^{-3}	XYZ
	detoc	mol m^{-3}	XYZ
$[\text{CaCO}_3]_{\text{calc}}$	calc	mol m^{-3}	XYZ
$[\text{CaCO}_3]_{\text{arag}}$	arag	mol m^{-3}	XYZ
~~$[\text{NH}_4^+]$ nh4 mol m^{-3} XYZ 2 Dissolved Ammonium Concentration~~ $[\text{CO}_3^{2-}]$	co3	mol m^{-3}	XYZ
$[\text{CO}_3^{2-}]^{\text{nat}}$	co3nat	mol m^{-3}	XYZ
$[\text{CO}_3^{2-}]^{\text{abio}}$	co3abio	mol m^{-3}	XYZ
$[\text{CO}_3^{2-}]_{\text{sat}}^{\text{calc}}$	co3satcalc	mol m^{-3}	XYZ
$[\text{CO}_3^{2-}]_{\text{sat}}^{\text{arag}}$	co3satarag	mol m^{-3}	XYZ

Table 12. Monthly mean biogeochemical output: Priority 3 (concentrations of surface fields)

Variable name	Units	Shape	Priority	Long name
baccos	mol m^{-3}	XY	3	Surface Bacterial Carbon Concentration
phydiatos	mol m^{-3}	XY	3	Surface Mole Concentration of Diatoms expressed as Carbon in sea water
phydiazos	mol m^{-3}	XY	3	Surface Mole Concentration of Diazotro...
phycalcos	mol m^{-3}	XY	3	Surface Mole Concentration of Calcareous Phytoplankton expressed as C...
phypicoos	mol m^{-3}	XY	3	Surface Mole Concentration of Picophytoplank...
phymiscos	mol m^{-3}	XY	3	Surface Mole Concentration of Miscellaneous Phytoplankton expressed a...
zmicroos	mol m^{-3}	XY	3	Surface...
zmesoos	mol m^{-3}	XY	3	Surface Mole Concentration of Mesozooplankton expressed as Carbon i...
zmiscos	mol m^{-3}	XY	3	Surface Mole Concentra...
chldiatos	kg m^{-3}	XY	3	Surface Mass Concentration of Diatoms expressed as Chlorophyll in sea...
chldiazos	kg m^{-3}	XY	3	Surface Mass Concentration of Diazotrophs expressed as Chlorophyll in...
chlcalcos	kg m^{-3}	XY	3	Surface Mass Concentration of Calc...
chlpicoos	kg m^{-3}	XY	3	Surface Mass Concentration of Picophytoplankton expressed as Chlorop...
chlmiscos	kg m^{-3}	XY	3	Surface Mass Concentration of Other...
ponos	mol m^{-3}	XY	3	Surface Mole Concentration of Particulate Organic Matter expressed as N...
popos	mol m^{-3}	XY	3	Surface Mole Concentration of Partic...
bfeos	mol m^{-3}	XY	3	Surface Mole Concentration of Particulate Organic Matter expressed as I...
bsios	mol m^{-3}	XY	3	Surface Mole Concentration of Particulate Organic Matter expressed as S...
phynos	mol m^{-3}	XY	3	Surface Mole Concentration of Phytoplankton Nitrogen in sea water
phypos	mol m^{-3}	XY	3	Surface Mole Concentration of Total Phytoplankton expressed as Phosph...
phyfeos	mol m^{-3}	XY	3	Surface Mass Concentration of Diazotrophs expressed as Chlorophyll in...
physios	mol m^{-3}	XY	3	Surface Mole Concentration of Total Phytoplankton expressed as Silicon...
dmsos	mol m^{-3}	XY	3	Surface Mole Concentration of Dimethyl Sulphide in sea water

Table 13. Monthly mean biogeochemical output: Priority 3 (concentrations ~~of 3-D fields~~)

Variable name	Units	Shape	Priority	Long name
bacc	mol m^{-3}	XYZ	3	Bacterial Carbon Concentration
phydiat	mol m^{-3}	XYZ	3	Mole Concentration of Diatoms expressed as Carbon in ~~Seawater~~sea water
phydiaz	mol m^{-3}	XYZ	3	Mole Concentration of Diazotrophs Expressed as Carbon in ~~Seawater~~sea water
phycalc	mol m^{-3}	XYZ	3	Mole Concentration of Calcareous Phytoplankton expressed as Carbon in ~~Seawater~~sea water
phypico	mol m^{-3}	XYZ	3	Mole Concentration of Picophytoplankton expressed as Carbon in ~~Seawater~~sea water
phymisc	mol m^{-3}	XYZ	3	Mole Concentration of Miscellaneous Phytoplankton expressed as Carbon in ~~Seawater~~sea water
zmicro	mol m^{-3}	XYZ	3	Mole Concentration of Microzooplankton expressed as Carbon in ~~Seawater~~sea water
zmeso	mol m^{-3}	XYZ	3	Mole Concentration of Mesozooplankton expressed as Carbon in ~~Seawater~~sea water
zmisc	mol m^{-3}	XYZ	3	~~Other Zooplankton Carbon Concentration~~Mole Concentraiton of Other Zooplankton expressed as Ca
chldiat	kg m^{-3}	XYZ	3	~~Diatom Chlorophyll Mass Concentration~~ Mass Concentration of Diatoms expressed as Chlorophyll i
chldiaz	kg m^{-3}	XYZ	3	Mass Concentration of Diazotrophs expressed as Chlorophyll in ~~Seawater~~sea water
chlcalc	kg m^{-3}	XYZ	3	Mass Concentration of Calcareous Phytoplankton expressed as Chlorophyll in ~~Seawater~~sea water
chlpico	kg m^{-3}	XYZ	3	Mass Concentration of Picophytoplankton expressed as Chlorophyll in ~~Seawater~~sea water
chlmisc	kg m^{-3}	XYZ	3	~~Other Phytoplankton Chlorophyll Mass Concentrationpoc mol m^{-3} XYZ 3 Particulate Organic Carb~~
pon	mol m^{-3}	XYZ	3	~~Particulate Organic Nitrogen Concentration~~Mole Concentration of Particulate Organic Matter expres
pop	mol m^{-3}	XYZ	3	~~Particulate Organic Phosphorus Concentration~~Mole Concentration of Particulate Organic Matter exp
bfe	mol m^{-3}	XYZ	3	~~Particulate Biogenic Iron Concentration~~Mole Concentration of Particulate Organic Matter expressed
bsi	mol m^{-3}	XYZ	3	~~Particulate Biogenic Silicon Concentration~~Mole Concentration of Particulate Organic Matter express
phyn	mol m^{-3}	XYZ	3	~~Phytoplankton Nitrogen Concentration~~Mole Concentration of Phytoplankton Nitrogen in sea water
phyp	mol m^{-3}	XYZ	3	~~Phytoplankton Phosphorus Concentration~~Mole Concentration of Total Phytoplankton expressed as P
phyfe	mol m^{-3}	XYZ	3	~~Phytoplankton Iron Concentration~~ Mass Concentration of Diazotrophs expressed as Chlorophyll in se
physi	mol m^{-3}	XYZ	3	~~Phytoplankton Silicon Concentration~~Mole Concentration of Total Phytoplankton expressed as Silicon
~~dms~~dmso	mol m^{-3}	XYZ	3	~~Dimethyl Sulphide Concentration~~Mole Concentration of Dimethyl Sulphide in sea water

Table 14. Monthly mean biogeochemical output: Priority 3 (gas exchange, river, burial, N_2 fixation, thresholds)

Symbol	Variable name	Units	Shape	Priority	Long name
$\Delta p\mathrm{CO}_2$	dpco2[*]	Pa	XY	3	Delta PCO2
$\Delta p\mathrm{CO}_2^{\mathrm{nat}}$	dpco2nat[*]	Pa	XY	3	Natural Delta PCO2
$\Delta p\mathrm{CO}_2^{\mathrm{abio}}$	dpco2abio[*]	Pa	XY	3	Abiotic Delta PCO2
$\Delta p\mathrm{O}_2$	dpo2[†]	Pa	XY	3	Delta PO2
F_{DMS}	fgdms	$\mathrm{mol\,m^{-2}\,s^{-1}}$	XY	3	Surface Upward Flux of DMS
	icfriver	$\mathrm{mol\,m^{-2}\,s^{-1}}$	XY	3	Flux of Inorganic Carbon Into Ocean Surface by Runoff
	fric	$\mathrm{mol\,m^{-2}\,s^{-1}}$	XY	3	Downward Inorganic Carbon Flux at Ocean Bottom
	ocfriver	$\mathrm{mol\,m^{-2}\,s^{-1}}$	XY	3	Flux of Organic Carbon Into Ocean Surface by Runoff
	froc	$\mathrm{mol\,m^{-2}\,s^{-1}}$	XY	3	Downward Organic Carbon Flux at Ocean Bottom
	intpn2	$\mathrm{mol\,m^{-2}\,s^{-1}}$	XY	3	Nitrogen Fixation Rate in Ocean
	fsn	$\mathrm{mol\,m^{-2}\,s^{-1}}$	XY	3	Surface Downward Net Flux of Nitrogen
	frn	$\mathrm{mol\,m^{-2}\,s^{-1}}$	XY	3	Nitrogen Loss to Sediments and through Denitrification
	fsfe	$\mathrm{mol\,m^{-2}\,s^{-1}}$	XY	3	Surface Downward Net Flux of Iron
	frfe	$\mathrm{mol\,m^{-2}\,s^{-1}}$	XY	3	Iron Loss to Sediments
	o2min	$\mathrm{mol\,m^{-3}}$	XY	3	Oxygen Minimum Concentration
	zo2min	m	XY	3	Depth of Oxygen Minimum Concentration
CSH	zsatcalc[‡]	m	XY	3	Calcite Saturation Depth
ASH	zsatarag[§]	m	XY	3	Aragonite Saturation Depth

[*] Difference between atmospheric and oceanic partial pressure of CO_2 (positive meaning ocean > atmosphere)

[†] Difference between atmospheric and oceanic partial pressure of O_2 (positive meaning ocean > atmosphere)

[‡] Depth of calcite saturation horizon (0 if < surface, "missing" if > bottom, if two, then the shallower)

[§] Depth of aragonite saturation horizon (0 if < surface, "missing" if > bottom, if two, then the shallower)

Table 15. Monthly mean biogeochemical output: Priority 3 (production and rates of change)

Variable name	Units	Shape	Priority	Long name
expn100[*]	mol m^{-2} s^{-1}	XY	3	Downward Flux of Particulate Nitrogen
expp100[*]	mol m^{-2} s^{-1}	XY	3	Downward Flux of Particulate Phosphorus
expfe100[*]	mol m^{-2} s^{-1}	XY	3	Downward Flux of Particulate Iron
expsi100[*]	mol m^{-2} s^{-1}	XY	3	Downward Flux of Particulate Silica
fddtdic[†]	mol m^{-2} s^{-1}	XY	3	Rate of Change of Net Dissolved Inorganic Carbon
fddtdin[†,‡]	mol m^{-2} s^{-1}	XY	3	Rate of Change of Net Dissolved Inorganic Nitrogen
fddtdip[†]	mol m^{-2} s^{-1}	XY	3	Rate of Change of Net Dissolved Inorganic Phosphorus
fddtdife[†]	mol m^{-2} s^{-1}	XY	3	Rate of Change of Net Dissolved Inorganic Iron
fddtdisi[†]	mol m^{-2} s^{-1}	XY	3	Rate of Change of Net Dissolved Inorganic Silicon
fddtalk[†]	mol m^{-2} s^{-1}	XY	3	Rate of Change of Total Alkalinity
fbddtdic[†]	mol m^{-2} s^{-1}	XY	3	Rate of Change of Dissolved Inorganic Carbon due to Biological Activity
fbddtdin[†,§]	mol m^{-2} s^{-1}	XY	3	Rate of Change of Dissolved Inorganic Nitrogen due to Biological Activity
fbddtdip[†]	mol m^{-2} s^{-1}	XY	3	Rate of Change of Total Dissolved Inorganic Phosphorus due to Biological Activity
fbddtdife[†]	mol m^{-2} s^{-1}	XY	3	Rate of Change of Dissolved Inorganic Iron due to Biological Activity
fbddtdisi[†]	mol m^{-2} s^{-1}	XY	3	Rate of Change of Total Dissolved Inorganic Silicon due to Biological Activity

[*] at 100-m depth

[†] integral over upper 100 m only

[‡] Net time rate of change of nitrogen nutrients (e.g. $NO_3^- + NH_4^+$)

[§] Vertical integral of net biological terms in time rate of change of nitrogen nutrients (e.g. $NO_3^- + NH_4^+$)

Table 16. Monthly mean biogeochemical output: Priority 3 (production, grazing, sinking, limitation)

| Variable name	Units	Shape	Priority	Long name
pp	mol m^{-3} s^{-1}	XYZ	3	Primary Carbon Production by Phytoplankton
graz	mol m^{-3} s^{-1}	XYZ	3	Total Grazing of Phytoplankton by Zooplankton
expc	mol m^{-2} s^{-1}	~~XYZ~~XY	3	Sinking Particulate Organic Carbon Flux
limndiaz	1	XY	3	Nitrogen limitation of Diazotrophs
limncalc	1	XY	3	Nitrogen limitation of Calcareous Phytoplankton
limnpico	1	XY	3	Nitrogen limitation of Picophytoplankton
limnmisc	1	XY	3	Nitrogen Limitation of Other Phytoplankton
limirrdiaz	1	XY	3	Irradiance limitation of Diazotrophs
limirrcalc	1	XY	3	Irradiance limitation of Calcareous Phytoplankton
limirrpico	1	XY	3	Irradiance limitation of Picophytoplankton
limirrmisc	1	XY	3	Irradiance Limitation of Other Phytoplankton
limfediaz	1	XY	3	Iron limitation of Diazotrophs
limfecalc	1	XY	3	Iron limitation of Calcareous Phytoplankton
limfepico	1	XY	3	Iron limitation of Picophytoplankton
limfemisc	1	XY	3	Iron Limitation of Other Phytoplankton
intppdiaz	mol m^{-2} s^{-1}	XY	3	Net Primary Mole Productivity of Carbon by Diazotrophs
intppcalc	mol m^{-2} s^{-1}	XY	3	Net Primary Mole Productivity of Carbon by Calcareous Phytoplankton
intpppico	mol m^{-2} s^{-1}	XY	3	Net Primary Mole Productivity of Carbon by Picophytoplankton
intppmisc	mol m^{-2} s^{-1}	XY	3	Net Primary Organic Carbon Production by Other Phytoplankton
intpbn	mol m^{-2} s^{-1}	XY	3	Nitrogen Production
intpbp	mol m^{-2} s^{-1}	XY	3	Phosphorus Production
intpbfe	mol m^{-2} s^{-1}	XY	3	Iron Production
intpbsi	mol m^{-2} s^{-1}	XY	3	Silica Production
intpcalcite	mol m^{-2} s^{-1}	XY	3	Calcite Production
intparag	mol m^{-2} s^{-1}	XY	3	Aragonite Production
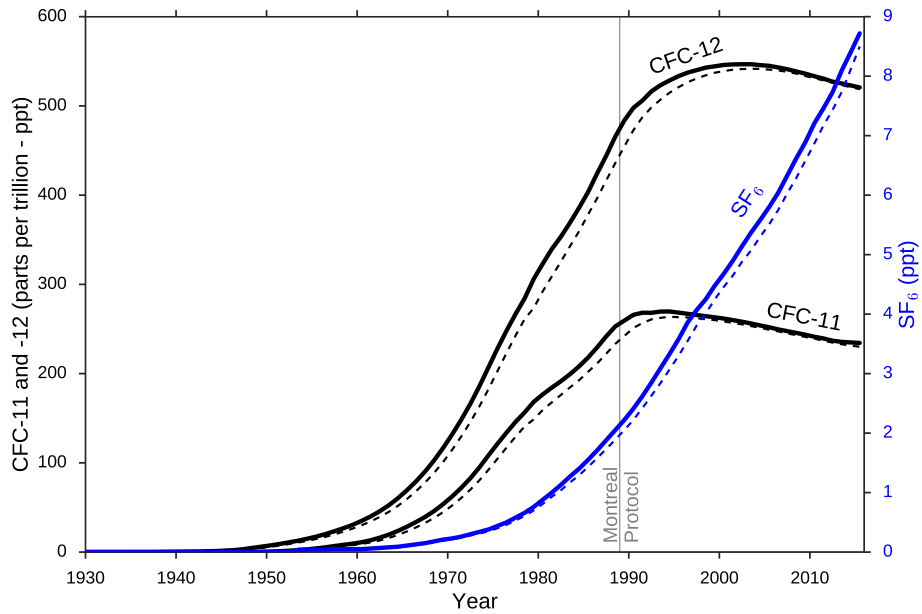
Figure 1. Histories of annual-mean tropospheric mixing ratios of CFC-11, CFC-12, and SF_6 for the northern hemisphere (solid line) and southern hemisphere (dashed line). Mixing ratios are given in parts per trillion (ppt) from mid-year data provided by Bullister (2015). For the OMIP simulations, these inert chemical tracers need not be included until the 4th CORE-II forcing cycle when they will be initialized to zero on 01 January 1936 (at model date 01 January 0237). The vertical grey line indicates the date when the Montreal protocol entered into force.
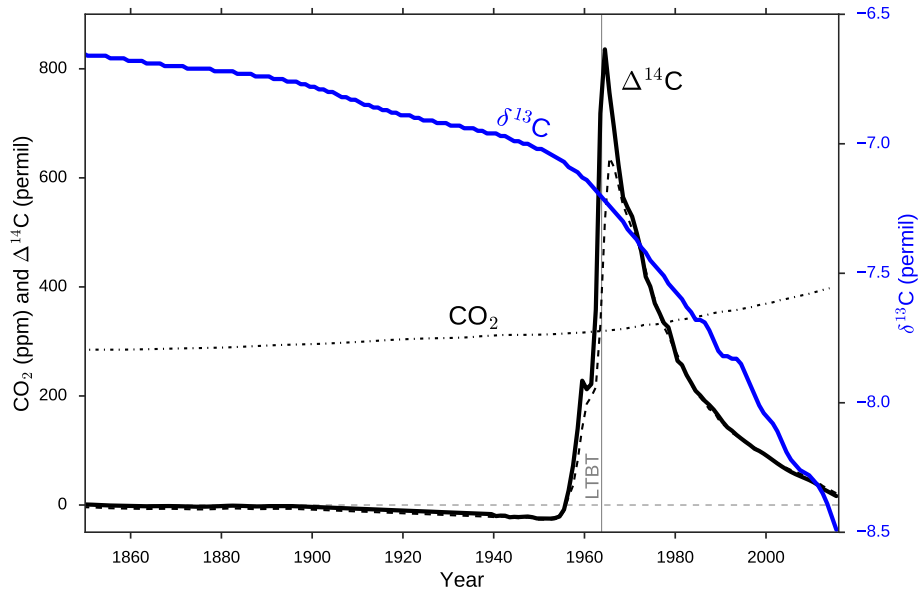
Figure 2. Annual-mean atmospheric histories for global-mean CO_2 (black dash-dot) and $\delta^{13}C$ (blue) compared to hemispheric means of $\Delta^{14}C$ for the north (black solid) and south (black dashes). The CO_2 data are identical to those used for CMIP6 (Meinshausen et al., 2016) and the carbon isotope data are common with C4MIP (Jones et al., 2016). The CO_2 observations are from NOAA (Dlugokencky and Tans, 2016) and Scripps Institution of Oceanography (Keeling et al., 2001), and $\delta^{13}C$ is a compilation of ice-core data (Rubino et al., 2013) and atmospheric measurements at Mauna Loa (Keeling et al., 2001). The $\Delta^{14}C$ data is compiled from Levin et al. (2010) and other sources. Data after 2009 are not used in OMIP Phase 1, but will be used in subsequent phases. Beyond 2009, atmospheric $\Delta^{14}C$ is unpublished data from the University of Heidelberg. Between the beginning of both OMIP simulations on 1 January 1700 and the same date in 1850, the atmospherc concentrations of CO_2, $\delta^{13}C$, and $\Delta^{14}C$ are to be held constant at are 285.375 ppm, -6.8‰ and 0‰, respectively. Also indicated are the preindustrial reference (0 permil) for atmospheric $\Delta^{14}C$ (horizontal grey dashed) and when the Limited Test Ban Treaty (LTBT) went into effect (vertical grey solid).
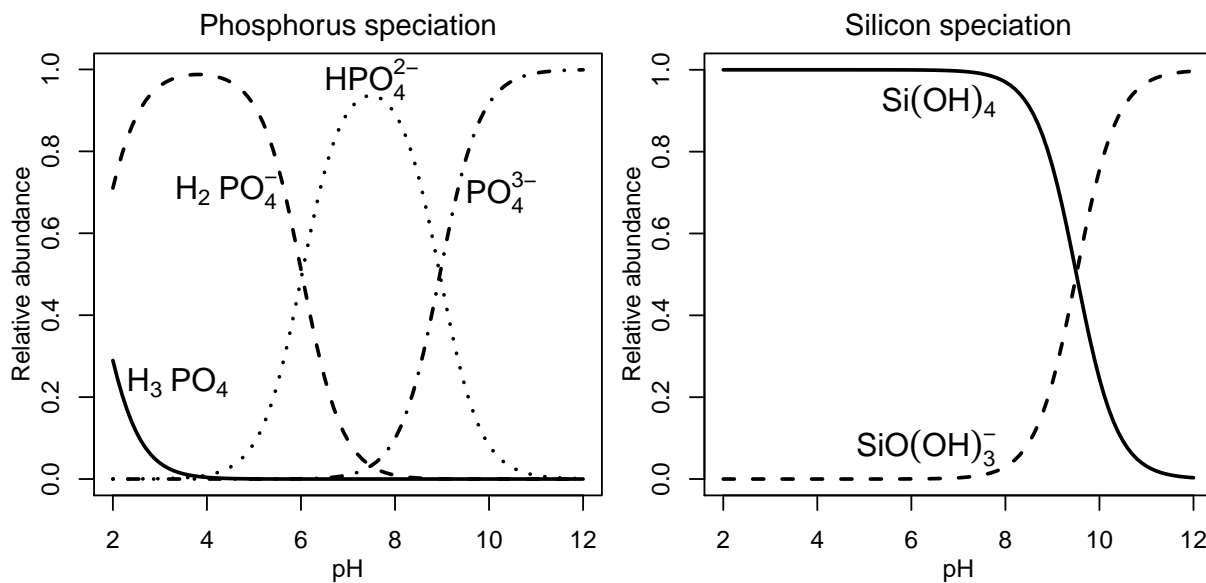
Figure 3. Relative molar abundance of inorganic species of phosphorus (left) and silicon (right) as a function of pH (total scale) in seawater at a temperature of $18°C$ and salinity of 35.